Master of Science Thesis

Signatures of Unparticle Self-Interactions at the Large Hadron Collider

Johannes Bergström

Theoretical Particle Physics, Department of Theoretical Physics
Royal Institute of Technology, SE-106 91 Stockholm, Sweden

Stockholm, Sweden 2009

Typeset in LaTeX

Examensarbete inom ämnet fysik för avläggande av civilingenjörsexamen inom utbildningsprogrammet Teknisk Fysik.

Graduation thesis on the subject Theoretical Physics for the degree of Master of Science in Engineering from the School of Engineering Physics.

TRITA-FYS 2009:03
ISSN 0280-316X
ISRN KTH/FYS/--09:03--SE

© Johannes Bergström, March 2009
Printed in Sweden by Universitetsservice US AB, Stockholm 2009

Abstract

Unparticle physics is the physics of a hidden sector which is conformal in the infrared and coupled to the Standard Model. The concept of unparticle physics was introduced by Howard Georgi in 2007 and has since then received a lot of attention, including many studies of its phenomenology in different situations.

After a review of the necessary background material, the implications of the self-interactions of the unparticle sector for LHC physics is studied. More specifically, analyses of four-body final states consisting of photons and leptons are performed. The results are upper bounds on the total cross sections as well as distributions of transverse momentum.

Keywords: unparticle physics, Large Hadron Collider (LHC), self-interactions, scale invariance, conformal invariance.

Sammanfattning

Opartikelfysik[1] handlar om fysiken som beskriver en dold sektor som är konform i den infraröda gränsen och kopplad till standardmodellen. Begreppet opartikelfysik introducerades av Howard Georgi år 2007 och har sedan dess fått mycket uppmärksamhet, vilket inkluderar studier av dess fenomenologi i många situationer.

Efter en genomgång av nödvändigt bakgrundsmaterial studeras innebörd av opartikelsektorns självväxelverkningar för fysik vid LHC. Mer specifikt så analyseras sluttillstånd med fyra partiklar bestående av leptoner och fotoner. Resultaten består av begränsningar på de totala tvärsnitten samt distributioner av transversell rörelsemängd.

Nyckelord: opartikelfysik, Large Hadron Collider (LHC), självväxelverkan, skalningsinvarians, konform invarians.

[1] Då ingen svensk text om denna modell är känd för författaren, introduceras härmed 'opartikelfysik' som översättning av engelskans 'unparticle physics'.

Preface

Unparticle physics is a relatively new idea, trying to extend the Standard Model of particle physics. It is essentially the physics of a quantum field theory having the conformal group as a symmetry group and interacting with the Standard Model. This thesis is structured as follows.

Chapter 1 is an introduction to this thesis where some remarks on physics in general and particle physics in particular is given. In Ch. 2, the basics of conformal field theory (CFT) is covered, starting with some elementary properties of the conformal group. After this, its implications for classical and quantum field theories having this group as a symmetry group are reviewed. The spectral density and propagator, which are essential for physical processes involving the conformal sector, are given a detailed treatment. For the specific results derived in this thesis, one also needs a good understanding of the three-point function and its Fourier transform. These are also investigated in this chapter and numerical results are given where appropriate. Also included is a review of the unitarity bounds which apply to the conformal sector and restrict its scaling dimension. Following this, the most well-known explicit examples of CFTs, the Banks-Zaks type theories, are described. Since the interactions with the Standard Model is necessarily described by an effective field theory, its basic principles will also be studied.

In Ch. 3, the unparticle model is described in more detail. The interactions with the standard model fields and the corresponding Feynman rules are given. The two most studied mechanisms through which the unparticle sector yields observable signals are creation of unparticle and propagator exchange. These are briefly discussed and then, finally, the breaking of conformal invariance in the unparticle sector and its implications for possible signatures are described.

In Ch. 4, the main results will be presented. These are a consequence of the unparticle self-interactions, entering through the three-point function and mediating processes with four-body final states at the LHC. First, an introduction to the physics at the LHC and the tools necessary to compute relevant observables are given. Then, the relevant squared amplitudes are calculated. Finally, upper bounds on cross sections and distributions of transverse momentum will be presented.

The thesis is concluded with Ch. 5, where the thesis and the results are summarized and some suggestions of further study are given.

Notation and Conventions

The metric tensor on Minkowski space $\mathbb{R}^{1,3}$ that will be used is

$$(g_{\mu\nu}) = \text{diag}(1, -1, -1, -1)$$

Dimensionful quantities will be expressed, in part, in units of $\hbar$ and c. Thus, one can effectively put $\hbar = c = 1$. As a result, both time and length are expressed in units of inverse mass,

$$[t] = T = M^{-1}, \qquad [l] = L = M^{-1}$$

- Also, the Einstein summation convention is employed, meaning that repeated indices are summed over, unless otherwise specified.

Acknowledgements

I would like to thank my supervisor Prof. Tommy Ohlsson for giving me the opportunity to do my thesis project at the Department of Theoretical Physics, for his guidance and support during my time at the department and for a thorough proofreading of this thesis. I would also like to thank Michal Malinský for giving me valuable input on the thesis. Thanks to everyone else at the department with whom I have had interesting discussions, especially Henrik Melbéus, Martin Sundin, Sofia Sivertsson, Jonas de Woul and He Zhang. Finally, i would like to thank my family, especially my parents for their constant support and my sister Elsa for being so joyful.

Contents

Chapter 1

Introduction

Physics, in its most general sense, is the study of the properties of the Universe. The goal of physics is to describe the various phenomena and properties of physical objects in terms of simpler, more fundamental phenomena. These more basic phenomena should then be described by even more fundamental ones. This process could potentially continue forever. At any given time one is then forced to conclude that the presently most fundamental phenomena are simply that and that there probably are even more basic ones which might or might not be found before the ultimate demise of the human species. If this process were to eventually end, the corresponding phenomena would have to in principle be able to describe all other appearing in the Universe. A theory describing these phenomena would be a *Theory of Everything* and are by some physicists considered the ultimate goal of physics, but by most a holy grail.

It is an amazing fact that the Universe supplies us with interesting physical phenomena on all accessible scales. From the age of the it (10^{18} s) to the lifetimes of heavy elementary particles (10^{-25} s). The study of the latter, the fundamental building blocks of the Universe which all other objects are composed of, is particle physics. In this sense, particle physics is *the* science which is the fundamental basis of all other sciences.

Since physics is a science, its practitioners should follow the *scientific method*. In its most basic form, it specifies the relation between experiment and theory and how a theory is supposed to be validated or falsified. For a theory to be scientific (or to be a theory at all) it must be *falsifiable*, i.e., it must be possible to conduct experiments which *disagree* with the predictions of the theory. The falsifiability should exist in *practise* and not only in principle. For example, the statement 'the Earth will explode in one billion years, plus or minus one day' is in principle falsifiable (one could just grab a chair, take a seat and start waiting), but not in practise.

For a theory to be a *valid* theory, its predictions should agree with the experimental data collected to date. Also, it should be able to make *new* predictions

which can be compared to future experimental data. It is important, however, to realize that the validity of a theory is defined only within a certain range or set of phenomena. A theory can be perfectly valid within one range but not within others. For example, non-relativistic classical mechanics is perfectly valid when all objects have small velocities compared to the speed of light, but not when they are comparable to it. Inherent in the above definition of a theory is the fact that a theory can never be *proofed* in a rigorous or tautological sense as theorems of mathematics can. Instead, it is based on certain assumptions or postulates, the validity of which can only be supported by the agreement of the theory's predictions with experiments.

Physical theories which agree extremely well with experimental results and disagree with them in no or very few instances are called *physical laws*. Note that a physical law is still a theory, just as theories which have been falsified are. In other words, the classification of something as a theory implies nothing whatsoever about its validity. This fact often causes great confusion among the general public, where a theory is often automatically thought of as something unverified or equivalent to an educated guess.

Another very important concept in science is *Occam's razor*, which in its most basic form states that a theory which makes fewer assumptions is to be preferred over one that makes more. In other words, when choosing between two descriptions of a set of phenomena, one should choose the simpler one (in the above sense) over the more complex one. In a way, Occam's razor can be thought of as a meta-theory, or theory of theories, which could, at least at first glance, be tested empirically. That is, if simpler theories turned out to have a higher degree of validity, Occam's razor would be a valid theory. It is also connected to the idea of falsifiability. A simple theory might be better simply because it uses less information to answer the same questions and is thus more easily falsifiable. A single sentence embodying Occam's razor but including an additional constraint (a paraphrase of a quote of Albert Einstein) is:

> "Make things as simple as possible, but not simpler."

It is in no way self-evident that that physical theories should be formulable using mathematics. However, this seems to be an empirical fact. This made Eugene Wigner make his famous comment on 'the unreasonable effectiveness of mathematics in the natural sciences'[1]:

> "The miracle of the appropriateness of the language of mathematics for the formulation of the laws of physics is a wonderful gift which we neither understand nor deserve. We should be grateful for it and hope that it will remain valid in future research and that it will extend, for better or for worse, to our pleasure, even though perhaps also to our bafflement, to wide branches of learning."

Einstein has also made a statement relating to this fact [2]:

> "The most incomprehensible thing about the world is that it is comprehensible."

Taken to its extreme limits, there have been suggestions that our physical universe might simply be an abstract mathematical structure [3]. However, the usefulness of mathematics seems to be smaller in some sciences different from physics such as biology, psychology and economics. For the case of biology, this made I. M. Gelfand state

> Eugene Wigner wrote a famous essay on the unreasonable effectiveness of mathematics in natural sciences. He meant physics, of course. There is only one thing which is more unreasonable than the unreasonable effectiveness of mathematics in physics, and this is the unreasonable ineffectiveness of mathematics in biology.

Today, the most well-established theory of the Universe on its most fundamental level is the *Standard Model* (SM) of particle physics. It describes all known fundamental particles and how they interact with each other. Gravity is not included in the SM, but is instead treated separately, usually using the general theory of relativity. Although it would be pleasant to have the SM and gravity unified, this does not matter in practise since there are no experimental circumstances where both the forces of the SM and gravity are relevant.

The SM is formulated as Quantum Field Theory (QFT), where each observable particle corresponds to a quantum field. The matter fields come in two groups: the *quarks* which have color charge and can interact via the so-called strong force and the *leptons* without color charge. Both of these come in three generations of doublets, i.e., there is a total of twelve types of matter particles plus their antiparticles. The fundamental forces are mediated through the *gauge bosons*: the photon, W- and Z-bosons and the gluons. Finally, there is the Higgs field which is responsible for the necessary breaking of the electroweak symmetry of the SM and the generation of the quark, charged lepton, W and Z masses. The Higgs particle is the only SM particle not yet observed. Despite the success of the SM, it has a number of shortcomings. These include the existence of neutrino masses, which are absent in the SM; the hierarchy problem, where there seems to be an unnaturally large cancellation between radiative corrections to the Higgs mass and its bare value; and finally, the non-existence of a dark matter candidate. This has lead theorists to try to extend the SM in various ways in order to resolve some of these problems. Unparticle physics, which is the topic if this theses, is one extension of the SM. However, it does not really try to solve any problems of the SM. Instead, the mere *possibility* of the existence of this extension is the motivation for its study. This, however, should not make it a 'worse' theory, since as explained in this introduction, it is finally experiments which should determine its validity.

A very good way to test theories of particle physics is to build machines, particle accelerators, that collide particles together and then observing what comes flying out in what directions and with what energies. One such is the Large Hadron

Collider (LHC). The LHC has been built in a circular tunnel 27 kilometers in circumference beneath the French-Swiss border near Geneva, Switzerland. When the LHC becomes fully operational, it will perform proton-proton collision at a center of mass energy of $\sqrt{s} = 14$ TeV. In the mean time, it is the job of the theorists to try to formulate the theories which are supposed to be tested and to calculate the predictions of these theories which can later be compared with LHC data. The final stage of relating theory to experiment is called *phenomenology*[1]. This thesis basically covers all the steps from formulating the theory or model (the extension of the SM) to the computation of observables at the LHC.

[1] Phenomenology in science in general has a different meaning, namely more that of results not derived from fundamental theory, but from more empirical considerations.

Chapter 2

Conformal Field Theory

Since unparticle physics is basically the physics of a conformal field theory (CFT) on Minkowski space coupled to the Standard Model (SM), it is wise to start with some basic properties of the conformal group and its implications regarding classical and quantum field theories. Although, in this thesis, we are really interested in conformal field theory on four-dimensional Minkowski space, the basics of conformal invariance will be explored in a general number of dimensions D, since this makes the bigger picture more clear.

Sometimes in quantum field theory on Minkowski space, one is confronted with calculations which cannot be evaluated as they stand. The common trick to use to obtain meaningful results (which might still be infinite) is to do the computations on Euclidean space with coordinates (x^4, x^1, x^2, x^3) instead. This is accomplished by performing a so-called *Wick rotation*, which is the simultaneous continuation to imaginary times and energies, $x^0 \to ix^4$, $k^0 \to ik^4$. This makes inner products transform into minus their Euclidean counterparts, $k \cdot x = k^0 x^0 - \overline{k} \cdot \overline{x} \to -(k^4 x^4 + \overline{k} \cdot \overline{x}) = -k \cdot x$ and $k^2 \to -k^2$. At the end of a calculation, one obtains the physical result on Minkowski space by simply performing the inverse of the Wick rotation. However, this often leads to undefined quantities due to poles, branch points or branch cuts on the real k^0 axis. To obtain well-defined quantities one needs to specify how these are to be handled. The correct way is to not rotate the entire way from the imaginary k^0 axis to the real, but instead to keep a small positive imaginary part for $\Re(k^0) > 0$ and a small negative imaginary part for $\Re(k^0) < 0$. This can be done by letting $k^0 \to k^0(1 + i\epsilon)$, which is in turn equivalent to taking $k^2 \to k^2 + i\epsilon$, the usual $i\epsilon$ prescription.

First, the conformal group is defined and some of its basic properties are investigated. Then an overview of its most relevant implication for classical as well as quantum field theory is presented. Following this is a detailed treatment of the spectral density, propagator and three-point function of a four dimensional CFT. Finally, unitarity bounds are presented and the most well-known examples of CFTs, the Banks-Zaks type theories, are briefly discussed.

2.1 The Conformal Group

Consider $\mathbb{R}^{p,q}$ with a flat metric $(g_{\mu\nu}) = \mathrm{diag}(\overbrace{1,\cdots,1}^{p},\overbrace{-1,\cdots,-1}^{q})$ and let $D = p+q$. Under a general change of coordinates, $x \mapsto x'$, the metric tensor transforms as

$$g_{\mu\nu}(x) \mapsto g'_{\mu\nu}(x') = \frac{\partial x^\alpha}{\partial x'^\mu}\frac{\partial x^\beta}{\partial x'^\nu} g_{\alpha\beta}(x).$$

The conformal group is defined as the group of invertible coordinate transformations leaving the metric invariant up to a local change of scale,

$$g_{\mu\nu}(x) \mapsto g'_{\mu\nu}(x') = \Omega(x) g_{\mu\nu}(x), \tag{2.1}$$

and thus preserving the 'angle'

$$\frac{a\cdot b}{\sqrt{a^2 b^2}}$$

between two vectors a and b. The Poincaré group is a subgroup of the conformal group, since it leaves the metric invariant.

To determine the nature of the transformations comprising the conformal group, one can study the infinitesimal coordinate transformations

$$x \mapsto x + \epsilon(x).$$

To first order in ϵ, the metric transforms as

$$g_{\mu\nu} \mapsto g_{\mu\nu} - (\partial_\mu \epsilon_\nu + \partial_\nu \epsilon_\mu).$$

Equation (2.1) now forces $(\partial_\mu\epsilon_\nu + \partial_\nu\epsilon_\mu)$ to be proportional to $g_{\mu\nu}$, while the constant of proportionality can be determined by tracing with $g_{\mu\nu}$, yielding

$$\partial_\mu \epsilon_\nu + \partial_\nu \epsilon_\mu = \frac{2}{d}\partial_\rho \epsilon^\rho g_{\mu\nu}. \tag{2.2}$$

If $D = 1$, there is no constraint on the transformation. Thus, any smooth coordinate transformation $\mathbb{R} \to \mathbb{R}$ is conformal. This is not very surprising, since there is no notion of an angle in this case. If $D = 2$, Eq. (2.1) implies either [4]

$$\partial_1 f^2 = \partial_2 f^1 \quad \text{and} \quad \partial_1 f^1 = -\partial_2 f^2$$

or

$$\partial_1 f^2 = -\partial_2 f^1 \quad \text{and} \quad \partial_1 f^1 = \partial_2 f^2.$$

Thus, writing $z, \overline{z} = x^1 \pm x^2$ and $f, \overline{f} = f^1 \pm f^2$, the conformal transformations are the holomorphic (or anti-holomorphic) functions, the local algebra of which

is infinite dimensional. However, demanding that the transformations are to be defined globally, the only allowed ones are the *projective transformations*

$$z \mapsto \frac{az+b}{cz+d}, \tag{2.3}$$

with $a, b, c, d \in \mathbb{C}$ and $ad - bc = 1$. Associating with each of these the matrix

$$\begin{pmatrix} a & b \\ c & d \end{pmatrix},$$

and letting the composition of two maps correspond to matrix multiplication, one observes that the global conformal group is isomorphic to $SL(2,\mathbb{C})/\mathbb{Z}_2$, where the quotient by $\mathbb{Z}_2$ is due to the invariance under $\{a, b, c, d\} \to \{-a, -b, -c, -d\}$. This is in turn isomorphic to $SO^+(3,1)$, the proper, orthochronous Lorentz group. A local field theory should, however, be sensitive to local symmetries. It is then the stringent constraints from local conformal symmetry that allow for the solutions of many two-dimensional conformal field theories.

Concentrating on the case $D \geq 3$, some manipulation of Eq. (2.2) yields

$$\partial_\nu \partial_\rho \partial_\sigma \epsilon_\mu = 0,$$

i.e., ϵ is at most quadratic in x. Without loss of generality, one can treat each power separately and order the different cases neatly as

$$\begin{aligned} \epsilon^\mu &= a^\mu, \\ \epsilon^\mu &= \omega^\mu{}_\nu x^\nu, \\ \epsilon^\mu &= \lambda x^\mu, \\ \epsilon^\mu &= b^\mu x^2 - 2x^\mu b \cdot x, \end{aligned}$$

corresponding to translations, Lorentz transformations (ω antisymmetric), dilations (scale transformations) and special conformal transformations (SCTs), respectively. Integration of these yields the finite transformations

$$\begin{aligned} x'^\mu &= x^\mu + a^\mu, \\ x'^\mu &= \Lambda^\mu{}_\nu x^\nu, \\ x'^\mu &= \lambda x^\mu, && \Omega(x) = \lambda^{-2}, \\ x'^\mu &= \frac{x^\mu + b^\mu x^2}{1 + 2b \cdot x + b^2 x^2}, && \Omega(x) = (1 + 2b \cdot x + b^2 x^2)^2. \end{aligned}$$

Note that since the SCT can be written as

$$\frac{x'^\mu}{x'^2} = \frac{x^\mu}{x^2} + b^\mu,$$

it is an inversion ($x \mapsto x/x^2$) followed by a translation ($x \mapsto x + b$) followed by another inversion.

2.2 Conformal Invariance in Classical Field Theory

Write a coordinate transformation and its action on a multicomponent field $\Phi(x)$ as

$$\begin{aligned} x &\mapsto, x' \\ \Phi(x) &\mapsto \Phi'(x') = \mathcal{F}(\Phi(x)). \end{aligned} \tag{2.4}$$

For an infinitesimal transformation with parameters $\{\omega_a\}$, this becomes

$$\begin{aligned} x' &= x + \omega_a \frac{\delta x}{\delta \omega_a}, \\ \Phi'(x') &= \Phi(x) + \omega_a \frac{\delta \mathcal{F}}{\delta \omega_a}(x). \end{aligned}$$

The *generators of infinitesimal transformations* G_a are in general defined as

$$-i\omega_a G_a = \Phi'(x) - \Phi(x).$$

Restricting our attention to the conformal transformations, one obtains the space-time part of the generators by requiring Φ to be a scalar under the conformal group, i.e., $\mathcal{F}(\Phi) = \Phi$. The result is

$$\begin{aligned} P_\mu &= -i\partial_\mu, \\ L_{\mu\nu} &= i(x_\mu \partial_\nu - x_\nu \partial_\mu), \\ D &= -ix^\mu \partial_\mu, \\ K_\mu &= -i\left(2x_\mu x^\nu \partial_\nu - x^2 \partial_\mu\right). \end{aligned} \tag{2.5}$$

These generators satisfy the *conformal algebra*:

$$\begin{aligned} [D, P_\mu] &= iP_\mu, \\ [D, K_\mu] &= -iK_\mu, \\ [K_\mu, P_\nu] &= 2i(g_{\mu\nu} D - L_{\mu\nu}), \\ [K_\rho, L_{\mu\nu}] &= i(g_{\rho\mu} K_\nu - g_{\rho\nu} K_\mu), \\ [P_\rho, L_{\mu\nu}] &= i(g_{\rho\mu} P_\nu - g_{\rho\nu} P_\mu), \\ [L_{\mu\nu}, L_{\rho\sigma}] &= i(g_{\nu\rho} L_{\mu\sigma} + g_{\mu\sigma} L_{\nu\rho} - g_{\mu\rho} L_{\nu\sigma} - g_{\nu\sigma} L_{\mu\rho}), \end{aligned}$$

while all other commutators vanish. Note that this yields the relation

$$e^{i\alpha D} P^2 e^{-i\alpha D} = e^{2\alpha} P^2, \tag{2.6}$$

implying that if dilation symmetry is exact, then either all masses are zero or the mass spectrum is continuous. If the tensor indices run from 1 to D, one can define

new antisymmetric generators J_{ab} with $a, b \in \{-1, 0, \cdots, D\}$ as

$$\begin{aligned} J_{\mu\nu} &= L_{\mu\nu}, \\ J_{-1\mu} &= \frac{1}{2}\left(P_\mu - K_\mu\right), \\ J_{0\mu} &= \frac{1}{2}\left(P_\mu + K_\mu\right), \\ J_{-10} &= D. \end{aligned}$$

These generators satisfy [5]

$$[J_{ab}, J_{cd}] = i(g_{bc}J_{ad} + g_{ad}J_{bc} - g_{ac}J_{bd} - g_{bd}J_{ac})$$

with $(g_{ab}) = \mathrm{diag}(-1, 1, \overbrace{1, \cdots, 1}^{p}, \overbrace{-1, \cdots, -1}^{q})$. Thus, the conformal group in $p+q$ dimensions is isomorphic to $SO(p+1, q+1)$. Note that since the Poincaré group augmented with dilations is a subgroup of the full conformal group, a relativistic field theory could, in principle, be scale but not conformally invariant.

To obtain the general transformation law for a multicomponent field under the conformal group, one needs to add finite dimensional matrix representations of the generators to the spacetime part in Eq. (2.5). Thus, in addition to the usual representations $S_{\mu\nu}$ (corresponding to spin) of $J_{\mu\nu}$, one also needs representations Δ of D and $\varkappa_\mu$ of K_μ. However, demanding that $S_{\mu\nu}$ forms an irreducible representation of the Lorentz algebra, Shur's lemma together with the conformal algebra imply that Δ is proportional to the identity,

$$\Delta = -id\mathcal{I}$$

for $d \in \mathbb{R}$, and that $\varkappa_\mu = 0$. The quantity d is called the *scaling dimension* of the field and is an important quantity in conformal field theory and will also be so in this thesis. One can now determine the transformation properties of a field with arbitrary spin under conformal transformations. The result for a Lorentz scalar $\phi(x)$ (with $S_{\mu\nu} = 0$) is

$$\phi'(x') = \left|\frac{\partial x'}{\partial x}\right|^{-d/D} \phi(x), \tag{2.7}$$

where $|\cdot|$ is the Jacobian. A field with the above transformation law is called *(quasi-)primary*.

Consider a function $\Theta(x_1, \cdots x_N)$ depending on N spacetime points $x_1, \cdots, x_N$. To determine its allowed form if it is required to be invariant under the full conformal group, start by observing that Poincaré invariance requires that Θ can only depend on the distances

$$r_{ij} = |x_i - x_j| .$$

Furthermore, invariance under dilations implies that there can only be dependence on the ratios

$$\frac{r_{ij}}{r_{kl}}.$$

Under a special conformal transformation the distance r_{ij} will become

$$r_{ij} \to r'_{ij} = \frac{r_{ij}}{\sqrt{(1+2b\cdot x_i + b^2 x_i^2)(1+2b\cdot x_j + b^2 x_j^2)}}.$$

Hence, only the $N(N-3)/2$ *cross-ratios*

$$\frac{r_{ij}r_{kl}}{r_{ik}r_{jl}} \tag{2.8}$$

will be invariant under all conformal transformations.

2.3 Conformal Invariance in Quantum Field Theory

Consider a collection of fields Φ, a Lagrangian density $\mathcal{L}$, which is a local expression in Φ and its derivatives, and the corresponding action

$$S[\Phi] = \int \mathrm{d}^D \mathcal{L}.$$

In quantum theory, one is interested in correlation functions or vacuum expectation values[1]

$$\langle \Phi(x_1)\cdots\Phi(x_n)\rangle = \frac{1}{Z}\int [\,\mathrm{d}\Phi]\,\Phi(x_1)\cdots\Phi(x_n)e^{iS[\Phi]},$$

where

$$Z = \int [\,\mathrm{d}\Phi]\, e^{iS[\Phi]}$$

is the vacuum functional and

$$\int [\,\mathrm{d}\Phi]$$

denotes functional integration.

A transformation which is a symmetry of the action is a symmetry of the classical theory. If the functional integration measure is invariant under the transformation[2], it is also a symmetry of the quantum theory, and one can easily derive the identity

$$\langle \Phi_1(x'_1)\cdots\Phi_n(x'_n)\rangle = \langle \mathcal{F}(\Phi_1(x_1))\cdots\mathcal{F}(\Phi_n(x_n))\rangle\,, \tag{2.9}$$

where $\mathcal{F}$ was defined in Eq. (2.4). For a field theory with conformal invariance, Eq. (2.7) implies that for two primary fields ϕ_1 and ϕ_2, the two-point function needs to satisfy

$$\langle \phi_1(x_1)\phi_2(x_2)\rangle = \left|\frac{\partial x'}{\partial x}\right|^{d_1/D}_{x=x_1}\left|\frac{\partial x'}{\partial x}\right|^{d_2/D}_{x=x_2}\langle \phi_1(x'_1)\phi_2(x'_2)\rangle\,. \tag{2.10}$$

[1] Which are time-ordered on Minkowski space.

[2] If it is not, the symmetry is said to be *anomalous*. This usually happens because the regularization procedure needed to define the theory properly does not respect the symmetry.

For scale transformations, $x \mapsto \lambda x$, this becomes

$$\langle \phi_1(x_1)\phi_2(x_2)\rangle = \lambda^{d_1+d_2} \langle \phi_1(\lambda x_1)\phi_2(\lambda x_2)\rangle .$$

Poincaré invariance then gives

$$\langle \phi_1(x_1)\phi_2(x_2)\rangle = \frac{C_{12}}{|x_1 - x_2|^{d_1+d_2}} \tag{2.11}$$

for some constant C_{12}. This, together with Eq. (2.10) and the fact that for SCTs

$$\left|\frac{\partial x'}{\partial x}\right| = \frac{1}{(1 + 2b\cdot x + b^2x^2)^D},$$

implies that

$$\frac{C_{12}}{|x_1 - x_2|^{d_1+d_2}} = \frac{(\gamma_1\gamma_2)^{(d_1+d_2)/2}}{\gamma_1^{d_1}\gamma_2^{d_2}} \frac{C_{12}}{|x_1 - x_2|^{d_1+d_2}}, \tag{2.12}$$

where

$$\gamma_i = 1 + 2b\cdot x + b^2x^2.$$

If Eq. (2.12) is to be an identity for arbitrary b, the factor containing the γ_i's needs to cancel. Hence, the fields must have the same scaling dimension to produce a nonzero result, i.e.,

$$\langle \phi_1(x_1)\phi_2(x_2)\rangle = \begin{cases} \frac{C_{12}}{|x_1-x_2|^{2d_1}} & \text{if } d_1 = d_2 \\ 0 & \text{if } d_1 \neq d_2 \end{cases} . \tag{2.13}$$

An example of two fields having the same scaling dimension could be a field $\phi_1 = \mathcal{O}$ and its Hermitian conjugate $\phi_2 = \mathcal{O}^\dagger$.

One can also find two-point functions for fields with arbitrary spin [6]. In general, the two fields must have the same scaling dimension and spin. For example, in four dimensions one finds [7]

$$\langle V_\mu(x_1)V_\nu(x_2)\rangle = C_V \frac{I_{\mu\nu}(x_1 - x_2)}{(r_{12}^2)^d}, \qquad I_{\mu\nu}(x) = g_{\mu\nu} - 2\frac{x_\mu x_\nu}{(x^2)^d}$$

for primary vector operators and

$$\langle T_{\mu\nu}(x_1)T_{\lambda\sigma}(x_2)\rangle = C_T \frac{\left(I_{\mu\lambda}(x_1 - x_2)I_{\nu\sigma}(x_1 - x_2) - \frac{1}{4}g_{\mu\nu}g_{\lambda\sigma}\right) \pm \mu \leftrightarrow \nu}{(r_{12}^2)^d}$$

for primary (anti)symmetric, traceless tensor operators.

An analysis similar to that performed for the two-point function can also be performed for the three-point function of three scalar fields. Poincaré invariance requires dependence on r_{12}, r_{13} and r_{23} only. Scale covariance then means

$$\langle \phi_1(x_1)\phi_2(x_2)\phi_3(x_3)\rangle = \int \mathrm{d}a\,\mathrm{d}b\,\mathrm{d}c \frac{C_{123}^{abc}}{r_{12}^a r_{23}^b r_{13}^c},$$

where, to obtain the correct total scaling, the integral (including a sum) is constrained by $a+b+c = d_1+d_2+d_3$. Covariance under special conformal transformations finally implies that the only allowed term is the one with

$$\begin{aligned} a &= d_1 + d_2 - d_3, \\ b &= d_2 + d_3 - d_1, \\ c &= d_1 + d_3 - d_2, \end{aligned} \tag{2.14}$$

i.e.,

$$\langle \phi_1(x_1)\phi_2(x_2)\phi_3(x_3)\rangle = \frac{C_{123}}{r_{12}^{d_1+d_2-d_3} r_{23}^{d_2+d_3-d_1} r_{13}^{d_1+d_3-d_2}}. \tag{2.15}$$

While scale covariance is enough to fix the two-point function for two fields with the same scaling dimension, a unique three-point function requires covariance under the full conformal group. In general, the three-point function can involve fields with different spin [6].

When moving on to higher-point functions, one has four or more points at one's disposal, and one can then construct totally invariant cross-ratios (cf. Eq. (2.8)), which the n-point function can have an arbitrary dependence on. For example, the four-point function has the general form

$$\langle \phi_1(x_1)\phi_2(x_2)\phi_3(x_3)\phi_4(x_4)\rangle = \rho\left(\frac{r_{12}r_{34}}{r_{13}r_{24}}, \frac{r_{12}r_{34}}{r_{14}r_{23}}\right) \prod_{i<j} r_{ij}^{\sum d_i/3 - d_i - d_j},$$

where ρ is an arbitrary function.

2.4 Correlation Functions in Momentum Space

In the computation of observables from the unparticle model, one usually needs the Fourier transform of the two-point function and the phase space, enetering through Feynman diagrams. In Ch. 4 the Fourier transform of the three-point function will also be needed. Thus, in this section, the above are calulated for a conformal field theory.

Define the Fourier transform $\Gamma(p_1, \cdots, p_{n-1})$ of the correlation functions of scalar fields as

$$\langle \phi_1(x_1) \cdots \phi_n(x_n) \rangle = \int \frac{\mathrm{d}^D p_1}{(2\pi)^D} \cdots \frac{\mathrm{d}^D p_{n-1}}{(2\pi)^D} \Gamma_n(p_1, \cdots, p_{n-1}) e^{-i \sum_i p_i \cdot x_i}.$$

There is no need to integrate over the last momentum variable, since it is fixed by translation invariance as $p_n = -(p_1 + \cdots + p_{n-1})$. By using Eq. (2.9), scale covariance directly implies

$$\Gamma_n(p_1, \cdots, p_{n-1}) = \lambda^{(n-1)D - \sum_i d_i} \Gamma(\lambda p_1, \cdots, \lambda p_{n-1}).$$

2.4.1 The Propagator

The *propagator*, which is the Fourier transform of the two-point function, of two fields with scaling dimension d thus has to have the form

$$\Gamma_2(p; d) = B_d (p^2)^{d - D/2} \tag{2.16}$$

for $B_d \in \mathbb{C}$. Considering only Minkowski space from here on, this becomes

$$\Gamma_2(p; d) = B_d (p^2)^{d-2}. \tag{2.17}$$

Note that this is the *full* (interacting) propagator[3], as opposed to the free one. From the form of this propagator, it is not hard to see that this corresponds to an *effective action* [8, 9]

$$S \sim \int \mathrm{d}^4 x \partial^\mu \phi \left(\partial^2\right)^{1-d} \partial_\mu \phi.$$

If possible, one would like to have more information about the propagator. First of all, the correct value of $(p^2)^{d-2}$ is given by choosing the principal value for the exponential together with $p^2 \to p^2 + i\epsilon$. One would also like to know the magnitude and phase of the constant B_d. These can be calculated by considering the unordered two-point function of $\mathcal{O}$ and $\mathcal{O}^\dagger$,

$$\langle 0 | \, \mathcal{O}(x) \mathcal{O}^\dagger(x') \, | 0 \rangle \, .$$

Using the fundamental property of the generators of translations, P_μ,

$$\mathcal{O}(x) = e^{iP \cdot x} \mathcal{O}(0) e^{-iP \cdot x}, \qquad P \, |0\rangle = 0$$

and inserting a complete set of states

$$1 = \int \mathrm{d}\lambda \, |\lambda\rangle \, \langle \lambda| \, ,$$

[3] At least before one couples the CFT to anything else.

one finds that

$$\langle 0|\,\mathcal{O}(x)\mathcal{O}^\dagger(x')\,|0\rangle = \int \mathrm{d}\lambda e^{-ip_\lambda\cdot(x-x')}\,|\langle 0|\,\mathcal{O}(0)\,|\lambda\rangle|^2\,,$$

where $P\,|\lambda\rangle = p_\lambda\,|\lambda\rangle$. Requiring the states to have non-negative masses[4], i.e., $p_\lambda^2, p_\lambda^0 \geq 0$ and then inserting

$$1 = \int_0^\infty \mathrm{d}s \int \mathrm{d}^4p\,\theta(p^0)\delta(s-p^2)\delta^{(4)}(p-p_\lambda),$$

one obtains

$$\langle 0|\,\mathcal{O}(x)\mathcal{O}(x')\,|0\rangle = \frac{1}{2\pi}\int_0^\infty \mathrm{d}s\rho(s)W(x-x';s), \tag{2.18}$$

where $W(x;s)$ is the unordered two-point function of a *free* field with mass $\sqrt{s}$,

$$W(x-x';s) = \int \frac{\mathrm{d}^4p}{(2\pi)^3}\theta(p^0)\delta(s-p^2)e^{-ip\cdot(x-x')}$$

and the *spectral density* $\rho(s)$ is formally given by

$$\rho(p^2) = (2\pi)^4 \int \mathrm{d}\lambda\delta^{(4)}(p-p_\lambda)\,|\langle 0|\,\mathcal{O}(0)\,|\lambda\rangle|^2\,.$$

Here $\rho(p^2)$ is obviously non-negative and it also contains a factor $\theta(p^2)\theta(p^0)$ by the assumptions $p_\lambda^2, p_\lambda^0 \geq 0$. Performing the integration with respect to s in Eq. (2.18), one finds

$$\langle 0|\,\mathcal{O}(x)\mathcal{O}^\dagger(x')\,|0\rangle = \int \frac{\mathrm{d}^4p}{(2\pi)^4}\rho(p^2)e^{-ip\cdot(x-x')}.$$

Now assume that $\mathcal{O}$ is conformally (scaling) covariant with scaling dimension d. Then $\langle 0|\,\mathcal{O}(x)\mathcal{O}(0)\,|0\rangle$ should have the same scaling as in Eq. (2.13), and hence $\rho(p^2)$ should have the same power law as the propagator, i.e.,

$$\rho(p^2) = A_d\theta(p^0)\theta(p^2)(p^2)^{d-2},$$

with the constant $A_d \geq 0$ by non-negativity of $\rho(p^2)$. Notice that, for integer $d \geq 1$, this would be the spectral density for d massless particles with total four-momentum p [10, 11] provided one makes the choice

$$A_d = \frac{16\pi^{5/2}}{(2\pi)^{2d}}\frac{\Gamma(d+\frac{1}{2})}{\Gamma(d-1)\Gamma(2d)}, \tag{2.19}$$

[4] Otherwise the vacuum would not be the vacuum.

where Γ is the gamma function. For $d \geq 2$ this is finite, while for $d \to 1^+$ the pole of the gamma function in the denominator gives

$$A_d \to 2\pi(d-1).$$

Thus, with $\epsilon = d - 1$ the spectral density in this limit becomes

$$\lim_{d\to 1^+} \rho(p^2; d) = 2\pi\theta(p^0)\theta(p^2) \lim_{\epsilon\to 0^+} \epsilon(p^2)^{\epsilon-1} = 2\pi\delta(p^2),$$

which is the density of a free massless field. One can now simply define A_d as the above expression for general d, which is basically a normalization of the field $\mathcal{O}$.

Using Eq. (2.18) and

$$\left\langle \mathcal{O}(x)\mathcal{O}^\dagger(x')\right\rangle = \theta(x^0 - x'^0) \left\langle 0\right| \mathcal{O}(x)\mathcal{O}^\dagger(x') \left|0\right\rangle + \theta(x'^0 - x^0) \left\langle 0\right| \mathcal{O}^\dagger(x')\mathcal{O}(x) \left|0\right\rangle \tag{2.20}$$

for the time-ordered vacuum expectation value, one easily finds

$$\left\langle \mathcal{O}(x)\mathcal{O}^\dagger(x')\right\rangle = \frac{1}{2\pi} \int_0^\infty \mathrm{d}s\rho(s) W^+(x - x'; s),$$

where

$$W^+(x - x'; s) = \int \frac{\mathrm{d}^4 p}{(2\pi)^4} \frac{e^{-ip\cdot(x-x')}}{p^2 - s + i\epsilon}$$

is the free field two-point function of a field with mass $\sqrt{s}$. Thus the propagator for $\mathcal{O}$, the Fourier transform of $\left\langle \mathcal{O}(x)\mathcal{O}^\dagger(x')\right\rangle$, is

$$\Gamma_2(p; d) = \frac{1}{2\pi} \int_0^\infty \mathrm{d}s\rho(s) \frac{1}{p^2 - s + i\epsilon} + \text{s.t.} \tag{2.21}$$

Here s.t. stands for any subtraction terms which might be needed if the integral does not converge in the ultraviolet (UV) region. This is related to the fact that, while Eq. (2.18) always exists in the distribution sense, in Eq. (2.20) one has multiplied this distribution with another one, the θ function, which might not be well defined. In this expression, one also sees explicitly how the required continuous mass spectrum, as commented after Eq. (2.6), appears.

The integrand scales as s^{d-3} for conformal fields in the UV region and will diverge for $d \geq 2$. In fact, when one proceeds and starts to calculate observables using the above (as described in Ch. 3), one sometimes finds singular behavior when $d \geq 2$. For example, the energy density at finite temperature and some cross sections are proportional to $(2 - d)$ [12,13]. This together with the *lower* bound on the scaling dimension from unitarity (cf. Sec. 2.5) implies that one usually restricts one's attention to the range $1 \leq d \leq 2$ for scalars.

The integral in Eq. (2.21) can be performed, with the result being [10, 11, 14]

$$\Gamma_2(p;d) = A_d \frac{1}{2\sin(d\pi)}(-p^2 - i\epsilon)^{d-2}, \tag{2.22}$$

where

$$(-p^2 - i\epsilon)^{d-2} = \begin{cases} (-p^2)^{d-2} = \left|p^2\right|^{d-2} & \text{if } p^2 < 0 \\ (p^2)^{d-2} e^{-id\pi} & \text{if } p^2 > 0 \end{cases}.$$

Since A_d is assumed to be real, this fixes the phase of the propagator, although the magnitude is arbitrary (corresponding to field normalization). The propagator is real and without branch cuts for spacelike p, $p^2 < 0$. One could apparently also obtain the same phase of the propagator by requiring it to be real on Euclidean space ($\sim G_d(p^2)^{d-2}, G_d \in \mathbb{R}$) and then performing a Wick rotation, giving $q^2 \to -q^2$, followed by choosing the correct branch, $q^2 \to q^2 + i\epsilon$. Using A_d as in Eq. (2.19) and its limit as $d \to 1^+$, one obtains the free field result

$$\lim_{d\to 1^+} \Gamma_2(p;d) = \frac{1}{p^2}$$

as one should.

The propagators for higher spin fields can also be calculated. For vector fields on Euclidean space one finds [7]

$$[\Gamma_2(k;d)]_{\mu\nu} = C(k^2)^{d-2}\left(g_{\mu\nu} - Y\frac{k_\mu k_\nu}{k^2}\right), \tag{2.23}$$

where

$$Y = \frac{2(d-2)}{d-1}.$$

The factor $(k^2)^{d-2}$ is given by scaling covariance, while Y is given, through the Fourier transform, by covariance under the SCTs. Similar remarks apply to the propagators of two-index tensors as well, although these expressions become cumbersome [7].

2.4.2 The Three-Point Function in Momentum Space

Calculation of the Fourier transform of the three-point function for a scalar conformal field requires a bit more care.[5] Equation (2.15) gives

$$\Gamma_3(p_1,p_2;d_1,d_2,d_3) = C_{123}\int \mathrm{d}^D x\, \mathrm{d}^D y \frac{1}{|x-y|^a |x|^b |y|^c} e^{-ip_1\cdot x} e^{-ip_2\cdot y} \tag{2.24}$$

[5] As mentioned in Sec. 2.3, full conformal covariance is required to yield a unique three-point function.

on Euclidean space, where a, b and c were defined in Eq. (2.14). Now insert the resolution of the identity in the form

$$1 = \int \mathrm{d}^D z \delta^{(D)}(z-(x-y)) = \int \frac{\mathrm{d}^D q}{(2\pi)^D} \mathrm{d}^D z e^{-iq\cdot(z-(x-y))},$$

yielding

$$\Gamma_3(p_1,p_2;d_1,d_2,d_3) = C_{123} \int \frac{\mathrm{d}^D q}{(2\pi)^D} \mathrm{d}^D x \, \mathrm{d}^D y \, \mathrm{d}^D z \frac{1}{|z|^a |x|^b |y|^c} \times e^{-iq(z-(x-y))} e^{-ip_1\cdot x} e^{-ip_2\cdot y}.$$

Here the three position space integrations simply yield three different propagators[6] of scaling dimensions $a/2, b/2$ and $c/2$, respectively (cf. Eq. (2.16)), which is the Fourier transform of Eq. (2.13)). Remaining is then a loop integral,

$$\Gamma_3(p_1,p_2;d_1,d_2,d_3) = C_{123} \int \frac{\mathrm{d}^D q}{(2\pi)^D} \Gamma_2(q;a/2)\Gamma_2(p_1-q;b/2)\Gamma_2(p_2+q;c/2), \quad (2.25)$$

which can be calculated using standard techniques. Start by introducing Feynman parameters as

$$\frac{1}{A_1^{m_1}\cdots A_n^{m_n}} = \int_0^1 \mathrm{d}x_1 \cdots \mathrm{d}x_n \delta(\sum x_i - 1) \frac{\prod x_i^{m_i-1}}{(\sum x_i A_i)^{\sum m_i}} \frac{\Gamma(\sum m_i)}{\prod \Gamma(m_i)}. \quad (2.26)$$

For the case at hand, one requires $n = 3$ and

$$\begin{aligned} A_1 &= q^2, & m_1 &= \frac{D}{2} - \frac{a}{2}, \\ A_2 &= (p_1-q)^2, & m_2 &= \frac{D}{2} - \frac{b}{2}, \\ A_3 &= (p_2+q)^2, & m_3 &= \frac{D}{2} - \frac{c}{2}. \end{aligned}$$

To be able to perform the momentum integral in Eq. (2.25), one needs to complete the square in the denominator of Eq. (2.26),

$$\sum A_i x_i = q^2 x_1 + (p_1-q)^2 x_2 + (p_2+q)^2 x_3 = l^2 + s\Delta,$$

where $s = (p_1+p_2)^2$ and

$$\begin{aligned} l &= q + x_3 p_2 - x_2 p_1, \\ \Delta &= x_1 x_2 \frac{p_2^2}{s} + x_1 x_3 \frac{p_1^2}{s} + x_2 x_3. \end{aligned}$$

[6] Up to overall real factors which are absorbed into C_{123}.

Equations (2.25) and (2.26) now yield

$$\Gamma_3(p_1,p_2;d_1,d_2,d_3) = C_{123}\int \frac{\mathrm{d}^D q}{(2\pi)^D}\,\mathrm{d}x_1\,\mathrm{d}x_2\,\mathrm{d}x_3\delta(x_1+x_2+x_3-1) \times \frac{x_1^{m_1-1}x_2^{m_2-1}x_3^{m_3-1}}{(l^2+s\Delta)^{m_1+m_2+m_3}}\frac{\Gamma(m_1+m_2+m_3)}{\Gamma(m_1)\Gamma(m_2)\Gamma(m_3)}.$$

The change of variables $q \to l$ gives a unit Jacobian, whereupon using

$$\int \frac{\mathrm{d}^D l}{(2\pi)^D}\frac{1}{(l^2+s\Delta)^n} = \frac{1}{(4\pi)^{D/2}}\frac{\Gamma(n-D/2)}{\Gamma(n)}\left(\frac{1}{s\Delta}\right)^{n-D/2}$$

with $n = m_1+m_2+m_3 = \frac{3D}{2} - \frac{1}{2}(a+b+c) = \frac{3D}{2} - \frac{1}{2}(d_1+d_2+d_3)$ finally gives the result

$$\begin{aligned}\Gamma_3(p_1,p_2;d_1,d_2,d_3) &= C_{123}K_{123} \\ &\times \left(\frac{1}{s}\right)^{D-\frac{1}{2}(d_1+d_2+d_3)}\int \mathrm{d}x_1\,\mathrm{d}x_2\,\mathrm{d}x_3\delta(x_1+x_2+x_3-1) \\ &\times \left(\frac{1}{\Delta}\right)^{D-\frac{1}{2}(d_1+d_2+d_3)} x_1^{m_1-1}x_2^{m_2-1}x_3^{m_3-1},\end{aligned}$$

where

$$K_{123} = \frac{\Gamma(D-\frac{1}{2}(d_1+d_2+d_3))}{(4\pi)^{D/2}\Gamma(m_1)\Gamma(m_2)\Gamma(m_3)}.$$

If $D = 4$ and all the fields ϕ_i have the same scaling dimension d, then $m_1 = m_2 = m_3 = 2 - d/2$ and one obtains

$$\Gamma_3(p_1,p_2;d) = C_d\left(\frac{1}{s}\right)^{4-3d/2} T_I\left(\frac{p_1^2}{s},\frac{p_2^2}{s}\right),$$

where

$$T_I\left(\frac{p_1^2}{s},\frac{p_2^2}{s}\right) = \frac{\Gamma(4-3d/2)}{\Gamma(2-d/2)^3}\frac{1}{(4\pi)^2}\int \mathrm{d}x_1\,\mathrm{d}x_2\,\mathrm{d}x_3\delta(x_1+x_2+x_3-1) \times \left(\frac{1}{\Delta}\right)^{4-3d/2}(x_1x_2x_3)^{1-d/2}.$$

The conversion to Minkowski space yields a factor of $-i$ and

$$\left(\frac{1}{s}\right)^{4-3d/2} \to \left(\frac{1}{-s-i\epsilon}\right)^{4-3d/2}$$

where now $s = (p_1+p_2)^2$ is positive in a scattering process, in which case the above is simply given by

$$\left(\frac{1}{s}\right)^{4-3d/2} e^{-i\frac{3d}{2}\pi}.$$

Since Δ remains unchanged, one has

$$\Gamma_3(p_1,p_2;d) = -ie^{-i\frac{3d}{2}\pi}C_d\left(\frac{1}{s}\right)^{4-3d/2} T_I\left(\frac{p_1^2}{s},\frac{p_2^2}{s}\right).$$

The integration with respect to one of the Feynman parameters, say x_3, can be done trivially due to the delta function, leaving an integration

$$\int_0^1 \mathrm{d}x_1 \int_0^{1-x_1} \mathrm{d}x_2 \cdots .$$

Now perform the change of variables

$$x_1 = 1-\omega, \qquad x_2 = \omega\rho$$

with Jacobian ω. The resulting integral is over the unit square and the integration with respect to ω can be done analytically, with the result being

$$\begin{aligned} T_I(A,B) = \frac{\Gamma(4-3d/2)}{\Gamma(2-d/2)^3}\frac{(1-d/2)}{16\pi\sin(\frac{d\pi}{2})}\int_0^1 \mathrm{d}\rho((1-\rho)\rho)^{1-\frac{d}{2}}\left(\frac{1}{A\rho+B-B\rho}\right)^{4-\frac{3d}{2}} \\ \times {}_2F_1\left[\frac{d}{2}, 4-\frac{3d}{2}, 2, \frac{A\rho+B-B\rho+\rho(\rho-1)}{A\rho+B-B\rho}\right] \end{aligned}$$

with ${}_2F_1$ the hypergeometric function. The integrand is singular at both endpoints, but with a good integration method, it can be integrated numerically. The result for different values of d are shown in Fig. 2.1. Just as the case was for the propagator, this is the exact three-point function. One also finds that T_I, and thus also $\Gamma_3(p_1,p_2;d)$, is symmetric in the momentum variables, as it should be by its definition in Eq. (2.24).

2.5 Unitarity Bounds

To determine what kind of states a quantum theory with a given spacetime symmetry group allows, one should classify all irreducible unitary representations with positive energy. For the Poincaré group, this was done in Wigner's seminal paper [15]. For the conformal group of four-dimensional Minkowski spacetime, they are labelled by a finite dimensional irreducible representation (j_1,j_2) of the Lorentz group, as well as the scaling dimension d [16]. There are five classes of representations with different Poincaré content $\{m,s\}$, where m is the mass and s the spin.

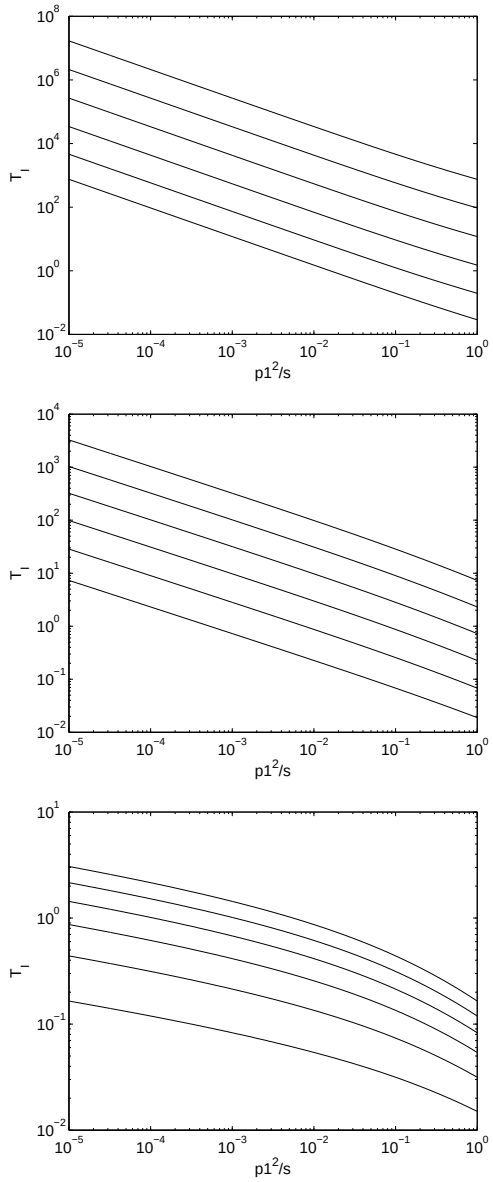

Figure 2.1. The function $T_I\left(\frac{p_1^2}{s}, \frac{p_2^2}{s}\right)$ for $d = 1.9$ (top), $d = 1.5$ (middle) and $d = 1.1$ (bottom). The values are shown as a function of p_1^2/s for the discrete values $p_2^2/s = 10^{-5}, 10^{-4}, 10^{-3}, 10^{-2}, 10^{-1}$ and 1 (from the top curves to the bottom ones).

Most importantly, the existence of these representations requires, by demanding that the unique inner product is positive semidefinite, that

$$d \geq j_1 + j_2 + 2 - \delta_{j_1 j_2, 0},$$

except for the trivial representation with $d = j_1 = j_2 = 0$. This translates into

$$\begin{aligned} d_S &\geq 1, \\ d_{Sp} &\geq \frac{3}{2}, \\ d_{T^-} &\geq 2, \\ d_V &\geq 3, \\ d_{T^+} &\geq 4 \end{aligned}$$

for Lorentz scalar, spinor, anti-symmetric tensor, gauge invariant vector and symmetric tensor operators, respectively. These constraints can also be obtained in a less formal setting by requiring unitarity of scattering amplitudes of particles coupled to the CFT and positivity of total cross sections using the optical theorem [7]. However, much of the phenomenology of unparticle physics dealing with vector and tensor operators are performed for values violating these bounds. This is usually circumvented by postulating only Poincaré and scale covariance instead of full conformal covariance. The problem with this assumption is that there are no known such four-dimensional QFTs [7] and it is quite possible that no such theories can exist. More information on the relation between scale and conformal invariance in different number of dimensions can be found in Ref. [17].

One also finds that the fields satisfy free field equations of motion and conservation laws if and only if the lower bounds are saturated. For vector and tensor operators, this includes the existence of zero-norm descendants

$$\partial_\mu V^\mu(x) = \partial_\mu T^{\mu\nu}(x) = 0.$$

In the unparticle physics literature, however, this together with scale covariance is usually postulated for general scaling dimensions instead of full conformal covariance. This is not only incompatible with conformal covariance, but also leads to different propagators for vector and tensor operators. For vectors, the result is Eq. (2.23), but with $Y = 1$ [11], which insures that

$$k^\mu \left[\Gamma_2(k; d)\right]_{\mu\nu} = 0.$$

2.6 Banks-Zaks Type Theories

In order for all the formalism presented so far to be of any use, one should be able to construct four-dimensional quantum field theories which possess covariance under the conformal group. The most famous nontrivial examples of such QFTs are

the theories of so-called Banks-Zaks [18] type. They will not be entirely conformal, however. Instead, they will be so only in the IR and UV limits but with two different scaling dimensions. In between, there is a transition between the two limits and no conformality.

Consider an $SU(N)$ gauge theory with N_f massless fermions in the representation R. The two-loop β function is[7] [19]

$$\beta(g) = -\beta_0 \frac{g^3}{(4\pi)^2} - \beta_1 \frac{g^5}{(4\pi)^4},$$

where the coefficients are

$$\begin{aligned} 2N\beta_0 &= \frac{11}{3} C_2(G) - \frac{4}{3} T(R), \\ (2N)^2 \beta_1 &= \frac{34}{3} C_2^2(G) - \frac{20}{3} C_2(G) T(R) - 4 C_2(R) T(R). \end{aligned}$$

Here $C_2(R)$ is the quadratic Casimir operator, normalized as

$$C_2(R) = N X_R^a X_R^a$$

with X_R^a the generators of R, whereas $T(R)$ is the trace normalization factor, related to $C_2(R)$ as

$$N_f C_2(R) d(R) = T(R) d(G),$$

where $d(R)$ is the dimension of the representation R and G denotes the adjoint representation.

At sufficiently small values of N_f, β_0 as well as β_1 will be positive. One then has QCD-like behavior with asymptotic freedom (vanishing coupling in the high-energy limit, i.e., a trivial UV fixed point) and strong coupling in the low energy (IR) limit. Since it is free in the UV limit, it will have its classical scaling dimension there.

If one keeps increasing the number of fermions, the second coefficient, β_1, will change sign at $N_f = N_f^{III}$ and a nontrivial IR stable fixed point, i.e., a zero of the β function, will emerge at $g = g_* \neq 0$. If this happens at a small value of the coupling, the theory will be conformal in the IR with a certain scaling dimension.

In general, however, when the coupling increases from high to low energy, before the coupling can reach g_*, it will reach the critical value g_c, where chiral symmetry is broken. This will lead to a $\langle \overline{\Psi}\Psi \rangle$ condensate, rendering the fermions massive. The fermions will then decouple from the dynamics and hence their screening effect will be lost. The fixed point g_* thus cannot be reached unless the number of fermions exceeds $N_f^{II} (\geq N_f^{III})$, which is the number of fermions required to make the coupling reach the fixed point before chiral symmetry is broken. The coupling then freezes at $g_* < g_c$ and chiral symmetry will remain intact.[8]

[7] This normalization of the group factors might be considered unusual.

[8] Another application of these types of gauge theories would be in *technicolor* models, where chiral symmetry breaking of a strongly coupled gauge theory is used to break the electroweak symmetry of the SM without the use of a Higgs field.

If one keeps increasing the number of fermions even more, the first coefficient, β_0, of the β function will change sign at $N_f = N_f^I (\geq N_f^{II})$. This will lead to a positive β function and loss of asymptotic freedom.

Using the fermions of this gauge theory, one can now construct gauge invariant operators with different tensor structures and parities. These will include the fermion bilinears

$$\mathcal{O}_\eta = \overline{\Psi}\eta\Psi$$

for η a combination of γ matrices. For example, one has scalar, vector and antisymmetric tensor operators [7]

$$\begin{aligned} \mathcal{O} &= \overline{\Psi}\Psi, \\ \mathcal{O}^\mu &= \overline{\Psi}\gamma^\mu\Psi, \\ \mathcal{O}^{\mu\nu} &= \overline{\Psi}\left[\gamma^\mu, \gamma^\nu\right]\Psi. \end{aligned} \tag{2.27}$$

These operators all have classical scaling dimensions equal to 3 (their mass dimension) which is then altered by quantum effects. In a gauge theory in the conformal window, they become conformal in the IR and at least the first two satisfy their respective unitarity bounds [7]. If one would rather have a non-composite operator as a conformal field, one can add a gauge singlet scalar field with classical scaling dimension at the unitarity bound $d_S = 1$, and then couple it to the fermions with a Yukawa coupling. This coupling also has a fixed point yielding a scaling dimension greater than one, consistent with the unitarity bound.

One can now define a scale $\Lambda_\mathcal{U}$, below which the theory is conformal.[9] If $\mathcal{O}_{UV}$ denotes any gauge invariant operator of the hidden sector with classical scaling dimension d_{UV} (such as those discussed above), it will undergo dimensional transmutation at the scale $\Lambda_\mathcal{U}$ and transform into a conformal operator $\mathcal{O}_\mathcal{U}$ with scaling and mass dimension d,

$$\mathcal{O}_{UV} \to (\Lambda_\mathcal{U})^{d_{UV}-d}\mathcal{O}_\mathcal{U}.$$

The nature of this transition is kind of obscure. In two dimensions one can find exact solutions of analogous models and observe the transition explicitly. The two-point function has the form $1/x^2$ in the UV (small distance) limit and $1/(x^2)^{1+a}$ in the IR (long distance) limit, where a can be given in terms of the parameters of the theory [21].

A similar analysis can also be performed for supersymmetric gauge theories. In fact, after introducing a measure in the parameter space of the gauge theories, one can calculate the fraction of asymptotically free gauge theories which are also conformal, i.e., one can calculate the 'size of the unparticle world' [22]. This fraction is exactly 0.5 and independent of the representation in the supersymmetric case, and approximately 0.25 in the nonsupersymmetric case.

[9] This will depend on convention, it can for example be defined as the scale where $g(\mu = \Lambda_\mathcal{U}) = \sqrt{\frac{2}{3}}g^*$ as in Ref. [20].

2.7 Principles of Effective Field Theory

Field theory textbooks usually argue that a QFT should be renormalizable, i.e., that the mass dimension of all the terms in the Lagrangian should be less than or equal to D, the dimensionality of spacetime. Otherwise one needs an infinite number of counterterms and hence an infinite number of unknown parameters, resulting in the loss of the predictive power of the theory.

An *effective* field theory Lagrangian, on the other hand, contains an infinite number of terms

$$\mathcal{L}_{EFT} = \mathcal{L}_{\leq D} + \mathcal{L}_{D+D_1} + \mathcal{L}_{D+D_2} + \cdots ,$$

where $\mathcal{L}_{\leq D}$ is the renormalizable Lagrangian and $\mathcal{L}_{D_i}$ contains terms of dimension D_i and $0 < D_1 < D_2 \cdots$. Although there is an infinite number of terms in $\mathcal{L}_{EFT}$, one still has *approximate* predictive power. Suppose Λ is the scale of some possibly unknown high-energy interactions. Then one can perform computations for processes at some scale $E < \Lambda$ with an error of $(E/\Lambda)^{D'}$ if one keeps terms up to $\mathcal{L}_{D+D'}$ in $\mathcal{L}_{EFT}$. Thus, an effective field theory is just as useful as a renormalizable one as long as one is satisfied with a certain finite accuracy.[10] This also means that the leading contribution for a given process at low energies is induced by the operators of lowest dimensionality. An operator appearing in an effective Lagrangian is usually called relevant, marginal or irrelevant if its dimension is less than, equal or larger than D. This is because the effect of an operator with dimensionality $D+D'$ is proportional to $(E/\Lambda)^{D'}$ and hence relevant/irrelevant operators are important/less important at low energies.

Given a renormalizable field theory involving a heavy field of mass M, one can integrate out the heavy field from the generating functional to produce an effective theory with an effective Lagrangian below M. For example, in QED one can integrate out the electron field to produce an effective Lagrangian, the Euler–Heisenberg Lagrangian

$$-\frac{1}{4}F^{\mu\nu}F_{\mu\nu} + \frac{a}{m_e^4}\left(F^{\mu\nu}F_{\mu\nu}\right)^2 + \frac{b}{m_e^4}F^{\mu\nu}F_{\nu\sigma}F^{\sigma\rho}F_{\rho\mu} + O\left(\frac{F^6}{m_e^8}\right),$$

where the dimensionless constants a and b can be found explicitly. However, even if one had no idea of what the high-energy theory was, one could still write down this unique Lagrangian (with unknown a and b, treated as free parameters) by simply imposing Lorentz, gauge, charge conjugation and parity invariance. In other words, the only effect of the high-energy theory is to give explicit values of the coupling constants in the low-energy theory. Exactly this property will be used in unparticle physics where the high-energy theory induces irrelevant operators involving the unparticle and SM field whose coupling constants will be treated as free parameters. For some more in-depth material on effective field theory, see Refs. [23, 24].

[10] The accuracy is usually finite anyway if one is using perturbation theory.

Chapter 3

Unparticle Physics

On the theoretical side, there has been a lot of research into the properties of conformal field theories. However, until recently the question of what the phenomenological consequences of the existence of a conformal hidden sector coupled to the Standard Model would be, had not been considered. The basic question that Georgi [10, 25] then asked was the following: suppose there existed a conformal field theory, for example of Banks-Zaks type (supersymmetric or not) in the IR, described in Sec. 2.6. What would then happen if it was coupled to the Standard Model, i.e., what would be the experimental signatures of the interaction between the hidden sector and the Standard Model? The couplings to the SM obviously have to be weak in some sense, since otherwise signatures of its existence would already have been discovered in experiments performed to date. If in addition one assigns SM quantum numbers to the unparticle field, even more stringent constraints will be imposed by current experimental data. An important point is also, that although the details of the physics of the hidden sector together with the SM will be very complicated, the low-energy physics will actually be simpler due to conformal covariance.

This chapter will start by a discussion of the basics of the unparticle model, including a description of some of the couplings to the SM and the corresponding Feynman rules. Next, the two most studied mechanisms of unparticle physics, production of unparticle and virtual unparticle exchange (through the propagator), are described. Finally, an introduction to the concept of conformal symmetry breaking of the conformal sector is given.

3.1 The Model

The basic scheme is the following. There is a hidden sector of Banks-Zaks type which couples to the Standard Model through a 'messenger field' with a large mass M, which simply means that both the SM and the hidden sector couple to this

field. Below the scale M, one can use effective field theory and integrate out the heavy field, whereby one ends up with effective operators suppressed by powers of M of the form[1]

$$c_n^i \frac{1}{M^{n+d_{UV}-4}} \mathcal{O}_n^i O_{UV}, \tag{3.1}$$

where c_n^i is a dimensionless constant and $\mathcal{O}_n^i$ and $\mathcal{O}_{UV}$ are local operators constructed out of the SM and hidden sector fields with mass dimensions n and d_{UV}, respectively. As discussed in Sec. 2.6, the hidden sector becomes conformal at the scale $\Lambda_\mathcal{U}$, for example by quantum effects via dimensional transmutation. The operator $\mathcal{O}_{UV}$ transitions into $(\Lambda_\mathcal{U})^{d_{UV}-d}\mathcal{O}_\mathcal{U}$, where $\mathcal{O}_\mathcal{U}$ has scaling and mass dimension d. This implies that the couplings of Eq. (3.1) have to be replaced by

$$c_n^i \frac{\Lambda_\mathcal{U}^{d_{UV}-d}}{M^{n+d_{UV}-4}} \mathcal{O}_n^i O_\mathcal{U} = \frac{c_n^i}{\Lambda_n^{n+d-4}} \mathcal{O}_n^i O_\mathcal{U}, \tag{3.2}$$

where the effective scale Λ_n given by

$$\Lambda_n^{n+d-4} = \frac{M^{n+d_{UV}-4}}{\Lambda_\mathcal{U}^{d_{UV}-d}}.$$

Note that $M, \Lambda_\mathcal{U}, d$ and d_{UV} are parameters of the messenger and hidden sector, while n will depend on what SM operator one is concerned with. Thus Λ_n will depend on n (and hence the subscript), i.e., operators of different mass dimension will couple with different strengths. In fact, these different energy scales counteract the effective field theory intuition that higher dimensional operators are more highly suppressed [26].

Note that the elimination of the heavy field will also induce contact interactions between generic SM fields $\mathcal{O}_{SM}$ such as

$$\mathcal{O}_{SM}^2 + \mathcal{O}_{SM}\partial^2\mathcal{O}_{SM} + \cdots,$$

suppressed by powers of M. These interactions have the potential to drown any unparticle effects [7] and thus could give the most stringent constraints on the parameter space relevant for unparticle physics.

3.2 Couplings to the Standard Model

In order to calculate observables, one needs explicit expressions for the couplings of the unparticle operators to the SM. Initially, the only constraint on the SM operator is that the interaction terms form Lorentz scalars. To reduce the number of possible interactions, one can assume that the unparticle operator is gauge invariant, and thus the SM operator has to be as well. All couplings of scalar, spinor and vector

[1] The notation will follow that of Ref. [26].

unparticle operators to gauge invariant SM operators with dimension less than or equal to four have been given in Ref. [27].

For a scalar unparticle field with scaling dimension d, the leading interaction with SM gauge bosons is through [26]

$$\frac{c_4^F}{\Lambda_4^d} F^a_{\mu\nu} F^{a\mu\nu} \mathcal{O} \tag{3.3}$$

and with fermions after electroweak symmetry breaking through

$$\frac{ec_4^f}{\Lambda_4^d} v \overline{f}_L f_R + \frac{ec_4^{f_{L,R}}}{\Lambda_4^d} \overline{f}_{L,R} \gamma_\mu f_{L,R} \partial^\mu \mathcal{O}_\mathcal{U}, \tag{3.4}$$

where the electromagnetic coupling has been pulled out for convenience. The first of these operators is proportional to v. Integrating the second one by parts, the vector contribution vanishes while the axial vector contribution is proportional to m_f. Since $m_f \ll v$ for all fermions except the top quark, the first interaction term will dominate for $c_4^f = O(c_4^{f_{L,R}})$.

For primary vectors, the interaction with SM fermions would be through

$$\frac{c_3^{f_{L,R}}}{\Lambda_3^{d-1}} \overline{f}_{L,R} \gamma_\mu f_{L,R} \mathcal{O}^\mu_\mathcal{U}$$

which would not be suppressed as the corresponding operator in Eq. (3.4). The vector cannot couple directly to gauge bosons since the number of uncontracted Lorentz indices will always be odd. It can, however, couple to them through a term like $H^\dagger D_\mu H \mathcal{O}^\mu$.

The Feynman rules for the interaction in Eq. (3.3) for photons and gluons and for the first one in Eq. (3.4) are thus

$$\begin{aligned} \mathcal{O}gg, \mathcal{O}\gamma\gamma \text{ vertex:} \qquad & V^{\mu\nu}(p_a, p_b) = i\frac{4c_{g,\gamma}}{\Lambda_4^d}(-p_a \cdot p_b g^{\mu\nu} + p_a^\nu p_b^\mu), \\ \mathcal{O}ff \text{ vertex:} \qquad & V = i\frac{ec_4^f}{\Lambda_4^d} v P_R, \end{aligned} \tag{3.5}$$

which will be used to study unparticle phenomenology in Ch. 4.

3.3 Production of Unparticle

One extremely important quantity in particle physics is the *cross section*, which is defined as the number of scattering events of a certain type normalized by the number of incoming particles per unit transverse area. It thus has the dimension of length squared and is usually measured in units of *barn* (or even fb or pb), $\mathrm{b} = 10^{-32}\,\mathrm{m}^2$. The outgoing particles also have specific directions, specified by

their momenta. The *differential* cross section is then defined in the same way as the cross section, but with the additional constraint that each particle should have a momentum in the 'volume element'

$$\frac{\mathrm{d}^3 p_n}{(2\pi)^3}\frac{1}{2E_n},$$

which is Lorentz invariant. In a scattering process with massless initial state particles having momenta p_1 and p_2 and final state particles having momenta $k_1, \ldots, k_n$, the differential cross section is

$$\mathrm{d}\sigma = \frac{1}{2s}\left|\mathcal{M}(p_1, p_2 \to k_1, \ldots, k_n)\right|^2 \mathrm{d}\Phi_n. \tag{3.6}$$

Here $s = (p_1 + p_2)^2$ and $\mathcal{M}(p_1, p_2 \to k_1, \ldots, k_n)$ is the amplitude for the given process. For a decay process where a particle with mass M' and momentum p_1 decays into particles with momenta $k_1, \ldots, k_n$, one instead has the *differential decay rate*

$$\mathrm{d}\Gamma = \frac{1}{2M'}\left|\mathcal{M}(p_1 \to k_1, \ldots, k_n)\right|^2 \mathrm{d}\Phi_n. \tag{3.7}$$

In these expressions $\mathrm{d}\Phi$ is the *phase space* given by

$$\mathrm{d}\Phi_n = (2\pi)^4 \delta^{(4)}(p_1 + p_2 - \sum_n k_n) \prod_n \frac{\mathrm{d}^3 p_n}{(2\pi)^3}\frac{1}{2E_n}. \tag{3.8}$$

If the some of the particles have other properties such as spin or color, $\mathrm{d}\sigma$ will depend on these. When one is only interested in the cross section independent of these properties, they are appropriately summed or averaged over in $|\mathcal{M}|^2$ to give $\overline{|\mathcal{M}|^2}$.

Since in the free field case the spectral density is

$$\rho_f(p^2; m) = 2\pi\theta(p^0)\delta(p^2 - m^2)$$

and the differential phase space volume in this case is

$$\frac{\mathrm{d}^3 p}{(2\pi)^3}\frac{1}{2p^0} = 2\pi\theta(p^0)\delta(p^2 - m^2)\frac{\mathrm{d}^4 p}{(4\pi)^2} = \rho_f(p^2; m)\frac{\mathrm{d}^4 p}{(4\pi)^2},$$

one adopts the differential phase space volume for creation of 'one' unparticle as

$$\rho(p^2)\frac{\mathrm{d}^4 p}{(4\pi)^2} = A_d\theta(p^0)\theta(p^2)(p^2)^{d-2}\frac{\mathrm{d}^4 p}{(4\pi)^2}.$$

This means that the unparticle can have any four-momentum p (given $p^0, p^2 \geq 0$), or equivalently any three-momentum and any mass.

Now suppose one has a scattering process in which n ordinary particles together with unparticle ($\mathcal{U}$) with four-momentum p are created,

$p_1, p_2 \to k_1, \ldots, k_n, p$. The differential cross section and decay rate are still given as above, but with the phase space now being [11]

$$\mathrm{d}\Phi_{n+\mathcal{U}} = (2\pi)^4 \delta^{(4)}(p_1 + p_2 - \sum_n k_n - p) \left(\prod_n \frac{\mathrm{d}^3 p_n}{(2\pi)^3} \frac{1}{2E_n} \right) \rho(p^2) \frac{\mathrm{d}^4 p}{(2\pi)^4} \tag{3.9}$$

For integer d, this would be the phase space for d massless particles simply because the spectral densities are the same in these cases. It is this correspondence that made Georgi claim that production of unparticle[2] stuff *looks* like production of a non-integral number d massless particles [10].[3] It is also this that made him name it 'unparticle stuff' in the first place, simply because it is *un*like *particle*s.

Using the phase space and different couplings to standard model fields one can start calculating physical observables. In Georgi's original paper [25], besides introducing the idea of unparticle physics, he calculated the energy spectrum of the u-quark in the decay process $t \to u\,\mathcal{U}$. He chose the effective interaction to be

$$i \frac{\lambda}{\Lambda^d} \overline{u} \gamma_\mu (1 - \gamma_5) t \partial^\mu \mathcal{O}_\mathcal{U} \; + \; \text{hermitian conjugate}$$

for scalar unparticle operator $\mathcal{O}_\mathcal{U}$ with scaling dimension d. The result he found was

$$\frac{1}{\Gamma} \frac{\mathrm{d}\Gamma}{\mathrm{d}E_u} = 4d(d^2 - 1)(1 - 2E_u/m_t)^{d-2} E_u^2 / m_t^2.$$

Thus the energy spectrum is continuous in the range $0 \leq E_u \leq m_t/2$ (and zero for $E_u \geq m_t/2$) in contrast to the monoenergetic spectrum which normally is present when there are two particles in the final state. As d approaches one from above, the spectrum becomes more and more peaked at $E_u = m_t/2$, reproducing the two-body result. Thus, in this limit the unparticle behaves as a single particle. The limit on unitarity, $d \geq 1$, expresses itself as a non-integrable singularity in $\frac{\mathrm{d}\Gamma}{\mathrm{d}E_u}$ for $d < 1$.

Quickly following this paper, other authors derived experimental signatures for a wide variety of other processes. Examples of such production processes are top decay ($t \to b\,\mathcal{U}$), fermionic Z decay ($Z \to f\overline{f}\,\mathcal{U}$), photonic Z decay ($Z \to \gamma\,\mathcal{U}$), Higgs decay ($H \to \gamma\,\mathcal{U}$), production at lepton colliders ($e^- e^+ \to (\gamma \text{ or } Z)\,\mathcal{U}$) and hadronic monojet production ($pp \text{ or } p\overline{p} \to (g, q \text{ or } \overline{q})\,\mathcal{U}$).

In these papers, it is generally assumed that the unparticle does not decay into SM particles. Thus, the unparticle will simply leave any detector undetected and lead to missing energy signals. However, the couplings to SM fields can through loops give a width to the unparticle propagator [29,30], so that the unparticle can, depending on model parameters, convert back into SM particles.

[2] Georgi used the term 'unparticle stuff' simply because it does not correspond to a fixed number of separate entities.

[3] However, in Ref. [28] it was shown that accounting for the interactions in the propagators of fermions and gauge bosons in gauge theories results in spectral densities for massless and massive particles that are virtually indistinguishable from those of unparticles.

3.4 Virtual Unparticle Effects

The coupling of SM fields to the unparticle field also gives rise to virtual unparticle effects, i.e., scattering processes proceeding via the unparticle propagator in Eq. (2.22). Not only will the different dependence on p^2 lead to unusual kinematical distributions, but the strange phase $e^{-id\pi}$ for timelike unparticle momenta[4] will lead to interference with the photon and Z-boson propagators. Examples of studied processes are dimuon ($e^+e^- \to \mu^+\mu^-$) and diphoton ($e^+e^- \to \gamma\gamma$) production at lepton colliders, the Drell-Yan process ($q\overline{q} \to l\bar{l}$) and diphoton production ($q\overline{q}$ or $gg \to \gamma\gamma$) at hadron colliders, photon-photon scattering ($\gamma\gamma \to \gamma\gamma$), decay and mixing of hadrons, neutrino physics and magnetic moments of leptons. For a mini-review of the phenomenology of unparticle physics including citations, see Ref. [31].

3.5 Conformal Symmetry Breaking

In Sec. 3.2, couplings of the hidden sector to SM gauge bosons and fermions were considered. Since the scaling dimension exceeds one and the SM operators all have mass dimension $n \geq 3$, these couplings are all irrelevant. There is, however, one additional type of coupling. This is the Higgs-unparticle coupling

$$\frac{1}{M^{d_{UV}-2}} H^\dagger H \mathcal{O}_{UV}.$$

In the IR, this becomes

$$\frac{\Lambda_{\mathcal{U}}^{d_{UV}-d}}{M^{d_{UV}-2}} H^\dagger H \mathcal{O}_{\mathcal{U}} = \frac{1}{(\Lambda_2)^{d-2}} H^\dagger H \mathcal{O}_{\mathcal{U}}.$$

For $d < 2$, this coupling is relevant and can significantly alter the low-energy physics of the unparticle sector. Once the Higgs field develops a vacuum expectation value (VEV) v (giving $H^\dagger H \to v^2$), this operator introduces a scale into the CFT[5] and will cause the theory to become non-conformal at the energy scale $\Lambda_{\not{\mathcal{U}}}$ [32], where

$$\Lambda_{\not{\mathcal{U}}}^{4-d} = \Lambda_2^{2-d} v^2.$$

Below the scale $\Lambda_{\not{\mathcal{U}}}$, the hidden sector presumably becomes a conventional particle sector. For consistency one requires $\Lambda_{\not{\mathcal{U}}} \leq \Lambda_{\mathcal{U}}$ and the two scales should also be reasonably well separated to give a window where the sector is conformal.

[4] The momentum of the virtual unparticle is timelike in s-channel processes and spacelike in u- and t-channel processes.

[5] It will also induce unparticle-Higgs mixing.

The standard way to incorporate the effect of conformal symmetry breaking into the CFT is to shift all the modes to higher energy by a certain amount $\mu \sim \Lambda_{\not U}$, i.e., to make the replacement

$$\rho(p^2) \to \rho_{\{\mu\}} = \rho(p^2 - \mu^2) = A_d \theta(p^0)\theta(p^2 - \mu^2)(p^2 - \mu^2)^{d-2}.$$

Thus, there are no states with $p^2 < \mu^2$ (a mass gap), above which there is a continuum. In the high-energy limit when $p^2 \gg \mu^2$, it matches the original density ρ. In the limit $d \to 1^+$, $\rho_\mu(p^2)$ approaches $\delta(p^2 - \mu^2)$, which is the spectral density of a free field with mass μ. There is, of course, also an identical shift in the propagator from Eq. (2.21), which becomes

$$\Gamma_2(p; d)_{\{\mu\}} = A_d \frac{1}{2\sin(d\pi)}(-p^2 + \mu^2 - i\epsilon)^{d-2}.$$

Supporting this ansatz is the fact, that using deconstruction in extra dimensions, the spectral function is shifted in this exact way [33]. In fact, it is also possible that, by coupling conformal right-handed neutrinos to the Higgs field, electroweak symmetry breaking can cause not only conformal symmetry breaking of the hidden sector, but also generation of neutrino masses [34].

Since typically $\Lambda_2 \sim v \sim 100\,\text{GeV}$, in the absence of fine tuning, the mass gap is at least a few GeV. This implies that there are no long range forces from unparticle exchange and that precision constraints (from the muon magnetic moment, for example) in practise disappear. Low-energy experiment are thus not sensitive to unparticle effects, and these are most easily probed at colliders. If the energy of the process in question is high enough, one can simply ignore mass gap in the propagator. In Ch. 4, the unparticle three-point function will be used to study possible signals at the LHC. Although it is unclear how to implement the breaking of conformal invariance into the three-point function, it is a reasonable assumption that one can ignore the existence of the mass gap as long as *all* the momentum invariants (q_1^2, q_2^2 and $(q_1 + q_2)^2$) in the three-point function are much larger than the conformal symmetry breaking scale. Since this will generally be the case at the LHC, this subject will not be discussed any further.

Chapter 4

LHC Phenomenology

In this chapter the main results of this thesis will be presented. These will be based on a unparticle-induced effect qualitatively different from those of unparticle production and effects mediated through the propagator (Secs. 3.3 and 3.4, respectively). This effect is the effect of unparticle *self-interactions*, first introduced by Feng, Rajarman and Tu [35][1], which for example can mediate processes with four-body final states at the LHC. While the authors of that paper considered the 4γ final state and the experimental bound on the unparticle self-interaction strength using Tevatron data, we will here consider also the $2\gamma 2l$ and $4l$ final states at the LHC, including those where two of the leptons are neutrinos.

First, an introduction to the physics at the LHC and the tools necessary to calculate relevant observables are given. Next, the squared amplitudes for the relevant processes are calculated. Finally, the main results, which are the p_T and $\not{p}_T$ spectra as well as the largest possible cross sections at the LHC, are presented.

4.1 Introduction to LHC Physics

When one calculates physical observables in high-energy physics processes, one usually calculates them by using the form of the interactions of elementary particles. For example, one might calculate the cross section for the process

$$q\overline{q} \to l^+ l^-.$$

However, since a proton is not an elementary particle, but instead a bound state of primarily quarks and gluons (collectively called *partons*), the availability of a method to extract measurable quantities from the fundamental interactions is crucial.

The QCD factorization theorem states that the cross section for high-energy hadronic processes can be factorized into the parton-level hard scattering cross

[1]The importance of the self-interactions of the hidden sector was also discussed in Ref. [36].

section convoluted with the so-called *parton distribution functions* (PDFs). In a scattering process with two hadrons A and B in the initial state and a final state F of interest, the cross section can be written as [37]

$$\sigma(AB \to F\,X) = \sum_{a,b} \int \mathrm{d}x_1\,\mathrm{d}x_2 P_{a/A}(x_1, Q^2) P_{b/B}(x_2, Q^2) \hat{\sigma}(ab \to F). \qquad (4.1)$$

Here X is the inclusive scattering remnant[2], $\hat{\sigma}(ab \to F)$ is the partonic cross section, $P_{a/A}$ is the PDF of parton a, x_i is the fraction of the hadron momentum carried by the corresponding parton and Q^2 is the factorization scale or typical momentum transfer in the hard scattering processes, which is to be much larger than the QCD scale $\Lambda^2_{QCD} \approx (200\mathrm{GeV})^2$ for the above to hold. The PDFs are determined using a combination of theoretical and experimental analyses and the most widely used are those of the CTEQ collaboration. In this thesis, the CTEQ6L [38] PDFs will be used.

The cross section only depends on the process in question and not on a specific experimental setup. In a real world experiment such as the LHC, what is measured is the number of events with certain properties. By the definition of the cross section, it and the number of events per unit time (R) are related by the number of particles that have passed each other per unit time transverse area, called the *luminosity* and denoted by $\mathcal{L}$,

$$R = \sigma\mathcal{L}.$$

The nominal luminosity of the LHC is about $100\,\mathrm{fb}^{-1}\,\mathrm{yr}^{-1}$[37].

When performing parton model calculations for hadron collisions using Eq. (4.1), the partonic CM frame is not the same as the hadronic one[3], simply because the two colliding partons have different fractions x_1 and x_2 of the hadron momenta. The partonic CM frame is boosted along the collision axis (the z-axis) in a random way given by the PDFs. In the massless limit, the phase space element can be written as

$$\frac{\mathrm{d}^3 p}{(2\pi)^3}\frac{1}{2E} = p_T\,\mathrm{d}p_T\,\mathrm{d}\phi\,\mathrm{d}\eta.$$

Here ϕ is the azimuthal angle (the angle in the xy-plane),

$$p_T = \sqrt{p_x^2 + p_y^2}$$

the *transverse momentum* (the momentum perpendicular to the collision axis) and

$$\eta = \ln\cot\frac{\theta}{2}$$

the *(pseudo-)rapidity*, where θ is the angle between the direction of the outgoing particle and the collision axis.

[2] All that is left when the remaining constituents of the protons have stopped interacting.
[3] This is usually and at the LHC the lab frame of the collider.

The total event rate at the LHC will be about 1 GHz [37]. Since a typical event will take about one megabyte of space, it is impossible to record all these events. Luckily, the majority of the events will not be interesting from a scientific point of view. The signals in the detector are compared with predefined limits on certain kinematical variables and the events are only recorded if they satisfy these limits. Cuts on η and p_T are very common and are effectively always imposed.

Equation for the partonic cross section and Eq. (4.1) for the inclusive one in pp collisions imply that the only thing one needs to be able to calculate observables at the LHC (except the PDFs) is the expression for the amplitude squared. This is where your specific theory or model comes in.

4.2 Unparticle Self-Interactions at the LHC

As discussed in Sec. 2.3, three- and higher-point functions are in general non-vanishing in conformal field theories. What is remarkable, is that the unparticle three-point function for fields such as in Eq. (2.27) does not necessarily vanish when the hidden sector gauge coupling goes to zero. In other words, even as the hidden gauge theory becomes free, the unparticles do not [36].

These higher-point functions can mediate processes such as

$$\Omega\overline{\Omega} \to \mathcal{U} \to \mathcal{U}\cdots\mathcal{U},$$

where Ω is any SM particle, $\overline{\Omega}$ its antiparticle and the number of unparticles are two or more. If the conformal sector is strongly coupled, the creation of an additional high-p_T unparticle does not suppress the rate.[4] This is in marked contrast to all known SM processes such as $gg \to g\cdots g$ and $gg \to \gamma\cdots\gamma$ where the addition of every high-p_T particle strongly suppresses the rate. This is because at energies well above $\Lambda_{QCD} \approx 200$ GeV, the entire SM is weakly coupled. The addition of a photon or gluon in the final state will reduce the cross section with factors of the order of $\frac{\alpha}{\pi} \approx 0.002$ and $\frac{\alpha_s}{\pi} \approx 0.02$ at LHC energies, respectively.

The natural choice when dealing with these kinds of self-interactions is to only consider the effects of the three-point function. This is because of two reasons. Firstly, as shown in Sec. 2.3, the three-point function is completely specified up to an overall constant by conformal invariance, while the four- and higher-point functions are not. Secondly, this is the leading order at which the resulting signal may be nearly background free.

While the unparticle propagator can give signals such as those mentioned in Sec. 3.4, the unparticle three-point function can induce processes such as

$$pp \to \mathcal{U} \to \mathcal{U}\mathcal{U} \to 4\gamma, 2\gamma 2l, 4l$$

[4] Only as long as one stays in the conformal regime. For processes with sufficiently high energy, the hidden sector will not be conformal.

and many other at the LHC. The basic parton-level Feynman diagrams are similar to the one shown in Fig. 4.1. The initial state can be either a gluon or a quark-antiquark pair, while the final state consists of two SM particle-antiparticle pairs, i.e., two of the pairs gg, $q\overline{q}$, W^+W^-, ZZ, $\gamma\gamma$, l^+l^-, $\nu\overline{\nu}$ and HH.

In principle, one could also couple SM particles to only one of the legs in the unparticle three-point function. This would lead to processes like

$$pp \to \mathcal{U} \to 2\gamma\,\mathcal{U}, l\bar{l}\,\mathcal{U}$$

with phase space for two particles and one unparticle (Eq. (3.9)). Since the phase space for the unparticle is so different, it cannot be easily integrated over numerically.

Note that, although the addition of unparticle lines from higher-point functions leads to no suppression, coupling of these to SM particles[5] does lead to suppression simply because the particle-unparticle coupling is small.

The main results of this thesis are extensions of results given in [35]. While the authors of that paper considered the 4γ final state and the experimental bound on the unparticle self-interaction strength using Tevatron data, we will here consider also the $2\gamma 2l$ and $4l$ final states at the LHC, including those where two of the leptons are neutrinos.

In order to calculate the cross section for these four-body final states, one needs to integrate over the momentum fractions in Eq. (4.1), a two-dimensional integration. In the integration over phase space in Eq. (3.8), each particle contributes a three-dimensional integration[6] and the δ-function conserving the total momentum reduces the total dimension by four. Also, one usually has cylindrical symmetry, rendering the integration over the azimuthal angle ϕ trivial. All integrations are over compact domains. For n particles in the final state, the total dimension of the necessary integration is thus

$$2 + 3n - 4 - 1 = 3n - 3,$$

which for a four-body final state equals 9. The integration over x_1 and x_2 always has to be performed numerically, since the PDFs are given as values on a lattice in $x_i - Q$ space. For two and three final state particles, the phase space integration can usually be done analytically, but for four this also has to be done numerically. The only tractable way to do this is to use Monte Carlo integration, which can be implemented as to perform all the integrations simultaneously. In producing the results of this thesis, the program CompHEP [39, 40] including the Monte Carlo integration algorithm VEGAS [41] has been used and slightly modified.

CompHEP is also able to perform event generation. One can look at the squared amplitude together with the PDFs and all the kinematical variables as defining a probability distribution in the $3n - 3$-dimensional space discussed above. The

[5] This one has to do in order to obtain detectable particles in the final state.

[6] Note that each unparticle requires a four-dimensional integration.

Monte Carlo program can subsequently generate a number of events, an event being represented by the momenta of all the particles participating in a reaction, according to this probability distribution. Using a list of many such events, one can analyze how they are distributed along different paths or surfaces in phase space. For example, one can plot the number of events as a function of the transverse momenta p_T.

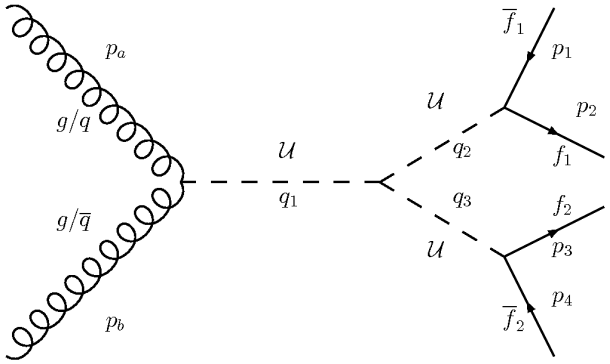

Figure 4.1. The Feynman diagram for the subprocesses $gg/q\overline{q} \to \mathcal{U} \to \mathcal{U}\mathcal{U} \to f_1\overline{f_1}f_2\overline{f_2}$.

4.2.1 General Amplitudes

Using the Feynman rules given in Eq. (3.5), one finds that the amplitudes for the processes in Fig. 4.1 are given by

$$i\mathcal{M} = \mathcal{M}_1(p_a, p_b)\mathcal{M}_2(p_1, p_2)\mathcal{M}_3(p_3, p_4)\Gamma_3(q_2, q_3),$$

where the $\mathcal{M}_i$ come from one vertex each. $\Gamma_3(q_2, q_3)$ is the Fourier transform of $\langle \mathcal{O}(x_1)\mathcal{O}(x_2)\mathcal{O}^\dagger(0)\rangle$, the computation of which is a special case of the one performed in Sec. 2.4.2 and plotted in Fig. 2.1. For external gauge bosons, the amplitude coming from one vertex is

$$\mathcal{M}_i(k_1, k_2) = \epsilon^1_\mu \epsilon^2_\nu V^{\mu\nu}(k_1, k_2),$$

where the polarization vectors ϵ^i_μ are conjugated if the gauge bosons appear in the final state. For initial and final state fermions, these are

$$\mathcal{M}_i(k_1,k_2) = \overline{v}(k_2)Vu(k_1) \quad \text{and} \quad \overline{u}(k_1)Vv(k_2),$$

respectively. Since each $\mathcal{M}_i$ is a scalar, one has

$$|\mathcal{M}|^2 = |\mathcal{M}_1(p_a,p_b)|^2 \, |\mathcal{M}_2(p_1,p_2)|^2 \, |\mathcal{M}_3(p_3,p_4)|^2 \, |\Gamma_3(q_2,q_3)|^2 \, .$$

Also, each $\mathcal{M}_i(k_1,k_2)$ only depends on the spins and colors of the particles with momenta k_1 and k_2, and hence for the spin and color average, one obtains

$$\overline{|\mathcal{M}|^2} = \overline{|\mathcal{M}_1|^2} \, \overline{|\mathcal{M}_2|^2} \, \overline{|\mathcal{M}_3|^2} \, |\Gamma_3(q_2,q_3)|^2 \, .$$

To calculate the averaged amplitudes, one uses

$$\sum_{\epsilon} \epsilon_\mu^* \epsilon_\nu \to -g_{\mu\nu}$$

for gauge bosons polarizations, giving

$$\sum_{\epsilon^1,\epsilon^2} |\mathcal{M}_i(k_1,k_2)|^2 = -V_{\mu\nu}(k_1,k_2)V^{\mu\nu}(k_1,k_2) = \frac{2^5 c_g^2}{\Lambda_4^{2d}}(k_1\cdot k_2)^2$$

For fermions, the identity for the summation over the particle spins that one needs is

$$\sum_{s_1,s_2} \left(\overline{r}(k_1)\Upsilon_1 t(k_2)\right)\left(\overline{r}(k_1)\Upsilon_2 t(k_2)\right)^* = \mathrm{Tr}\left[\Upsilon_1(\not{k}_2 \pm m_2)\gamma^0\Upsilon_2^\dagger\gamma^0(\not{k}_1 \pm m_1)\right],$$

where Υ_i are arbitrary matrices, and $r,t = u$ or v, giving plus and minus signs in front of the masses, respectively. Choosing $m_1 = m_2 = 0, \Upsilon_1 = \Upsilon_2 = V$ and performing the trace yields

$$\sum_{s_1,s_2} |\mathcal{M}_i(k_1,k_2)|^2 = 2\left(\frac{ec_4^f v}{\Lambda_4^d}\right)^2 k_1\cdot k_2. \tag{4.2}$$

The last thing one needs to obtain $\overline{|\mathcal{M}|^2}$, is to include the appropriate factor for averaging of the initial state colors and spins. Since there are eight different gluons and each gluon has two different polarizations, for a gg initial state one needs to include a factor of

$$\frac{1}{2}\cdot\frac{1}{2}\cdot\frac{1}{8} = \frac{1}{32}.$$

Since there are three colors of quarks, and they also have two different spin states, one includes a factor of

$$\frac{1}{2}\cdot\frac{1}{2}\cdot\frac{1}{3} = \frac{1}{12}$$

for a $q\overline{q}$ initial state.

For leptons and photons in the final state, there are six different squared amplitudes, corresponding to the different subprocesses

$$gg, q\overline{q} \to \gamma\gamma\gamma\gamma, \gamma\gamma l\overline{l}, l_1\overline{l}_1 l_2\overline{l}_2.$$

When calculating observables, the convention is to set $c_g = c_\gamma = 1$ and $e^2(c_4^f)^2 = 2\pi$ [26, 42]. Following Ref. [35], the reference values $C_d = 1$ and $\Lambda_4 = 1$ TeV will be chosen. It is easy to see that all cross sections will be proportional to C_d^2/Λ_4^{6d}. Because of the unitarity bound $d \geq 1$ and the more practical bound $d < 2$ discussed previously in this thesis, only this range on the scaling dimension will be considered. More specifically, the values $d = 1.1, 1.5$ and 1.9 will be used as representatives, hopefully giving a picture of the resulting differences caused by the different scaling dimensions in the chosen range.

4.2.2 Four Photon Final States

Following the general arguments given above, one finds that the squared amplitudes for the $gg \to \gamma\gamma\gamma\gamma$ and $q\overline{q} \to \gamma\gamma\gamma\gamma$ subprocesses are

$$\overline{|\mathcal{M}_{gg\to 4\gamma}|^2} = 2^{10}\frac{c_g^2 c_\gamma^4}{\Lambda_4^{6d}}(p_a\cdot p_b)^2(p_1\cdot p_2)^2(p_3\cdot p_4)^2\left|\Gamma_3(q_2,q_3)\right|^2,$$

$$\overline{|\mathcal{M}_{q\overline{q}\to 4\gamma}|^2} = \frac{2^9}{3}\frac{c_\gamma^4 e^2(c_4^f)^2}{\Lambda_4^{6d}}v^2(p_a\cdot p_b)(p_1\cdot p_2)^2(p_3\cdot p_4)^2\left|\Gamma_3(q_2,q_3)\right|^2,$$

respectively. These expressions do not include the factor of $1/4!$ needed to compensate for the overcounting caused by the integration over phase space for four identical particles.

By dimensional analysis, the total partonic cross sections are

$$\hat{\sigma}(\hat{s})_{gg\to 4\gamma} = f_d^g C_d^2\left(\frac{\hat{s}}{\Lambda_4}\right)^{3d}\frac{1}{\hat{s}/[\mathrm{GeV}^2]}[\mathrm{fb}],$$

$$\hat{\sigma}(\hat{s})_{q\overline{q}\to 4\gamma} = f_d^q C_d^2\left(\frac{\hat{s}}{\Lambda_4}\right)^{3d}\left(\frac{v^2}{\hat{s}}\right)\frac{1}{\hat{s}/[\mathrm{GeV}^2]}[\mathrm{fb}],$$

where f_d^g and f_d^q are dimensionless factors which can be extracted from the Monte Carlo integration and are given in Table 4.2.2 for different values of d.

To determine the LHC cross section, one starts to integrate over the PDFs and phase space. The final state photons are ordered with respect to their transverse momentum and required to satisfy

$$p_T^i > 30, 25, 15, 15\ \mathrm{GeV}, \quad \left|\eta^i\right| < 2.5 \tag{4.3}$$

for $i = 1, 2, 3, 4$. The resulting reference cross sections for $C_d = 1$ and $\Lambda_4 = 1$ TeV are given in Table 4.2.2. As explained in Sec. 4.2.3, Tevatron measurement

gives constraint on C_d/Λ_4^{3d}. Multiplying the reference cross section by this number squared yields upper bounds on the LHC cross sections, LHC $\sigma_{4\gamma}^{\max}$, which can also be found in Table 4.2.2. Note that the nominal LHC luminosity yields 10^5 events per year if the cross section is 10^3 fb and of course 10^8 events per year if the cross section is 10^6 fb.

After having generated a large number of events, one can order them according to their transverse momenta. The number of events as a function of p_T is shown in Fig. 4.2. These spectra are for the gg initial state only. However, after having generated p_T-spectra for a sample of $q\overline{q}$ initial states and values of d, one finds almost perfect agreement with the spectra from the gg initial state. Thus, if for some reason the unparticle field does not couple to gluons at all, the resulting spectra would be virtually identical although the total cross sections would be different.

As discussed in the beginning of this chapter, the SM background for the 4γ channel is expected to be small. Thus, if there was to be an excess of four photon events at the LHC, these distributions could possibly be used to identify unparticles as the source, as well as the correct value of the scaling dimension d. All the p_T-distributions can be seen to be reasonably hard for $d = 1.9$, while they become softer as d decreases towards 1.

Since there is no distinction between the couplings to photons and gluons, the p_T-distributions of gluons (measured as in four jet) would be identical to the ones for photons. Although the total cross section will be larger in this case due to the multiple colors of the gluons, the large QCD background will probably mask these signals completely.

4.2.3 Tevatron Bounds

In order to give bounds on the cross sections of processes mediated by unparticle self-interactions, one needs bounds on the constant C_d appearing in the three-point function which determines the strength of the self-interaction. However, there is no known way to do this theoretically and thus one needs to turn to experiment. These bounds could come from any collider experiment. Since there is no LHC data available yet, it is natural to turn to the Tevatron. Only the bounds from the 4γ channel calculated in Ref. [35] will be used in this thesis.

No excess of events beyond the SM prediction was found using data collected at the D0 detector during 2002-2005 with $0.83 \pm 0.05\text{fb}^{-1}$ of integrated luminosity [43]. The SM background at the Tevatron can be estimated as [35]

$$\sigma_{q\overline{q}\to 4\gamma}^{SM} \approx \left(\sum_q Q_q\right)\left(\frac{\alpha}{\pi}\right)^2 \sigma_{q\overline{q}\to 2\gamma}^{SM} \approx 3 \cdot 10^{-3} \text{ fb}$$

and a similar estimation should apply to the LHC. The resulting cross section will change because of two reasons. These are the different energies and the fact that

	$d = 1.1$	$d = 1.5$	$d = 1.9$
f_d^g	3.0	0.17	0.021
f_d^q	6.3	0.35	0.044
h_d^g	390	8.1	0.79
h_d^q	830	17	1.7
j_d^g	560	6.7	0.57
j_d^q	1200	14	1.2
Tevatron bounds on $C_d/(\Lambda_4\ [\mathrm{TeV}])^{3d}$	1.3×10^4	1.2×10^5	4.8×10^5
LHC $\sigma^{\mathrm{ref}}_{gg\to 4\gamma}$ [fb]	2.9×10^{-5}	1.1×10^{-5}	3.2×10^{-5}
LHC $\sigma^{\mathrm{ref}}_{q\overline{q}\to 4\gamma}$ [fb]	$1.0 \cdot 10^{-6}$	$3.8 \cdot 10^{-7}$	$1.1 \cdot 10^{-6}$
LHC $\sigma^{\mathrm{max}}_{4\gamma}$ [fb]	$5.0 \cdot 10^3$	$1.7 \cdot 10^5$	$7.6 \cdot 10^6$
LHC $\sigma^{\mathrm{ref}}_{gg\to 2l2\gamma}$ [fb]	$1.9 \cdot 10^{-4}$	$5.7 \cdot 10^{-6}$	$5.1 \cdot 10^{-6}$
LHC $\sigma^{\mathrm{ref}}_{q\overline{q}\to 2l2\gamma}$ [fb]	$1.0 \cdot 10^{-5}$	$2.0 \cdot 10^{-7}$	$1.7 \cdot 10^{-7}$
LHC $\sigma^{\mathrm{max}}_{2l2\gamma}$ [fb]	$3.4 \cdot 10^4$	$8.5 \cdot 10^4$	$1.2 \cdot 10^6$
LHC $\sigma^{\mathrm{ref}}_{gg\to 4l}$ [fb]	$1.1 \cdot 10^{-4}$	$1.9 \cdot 10^{-7}$	$3.2 \cdot 10^{-8}$
LHC $\sigma^{\mathrm{ref}}_{q\overline{q}\to 4l}$ [fb]	$1.1 \cdot 10^{-5}$	$9.3 \cdot 10^{-9}$	$1.1 \cdot 10^{-9}$
LHC $\sigma^{\mathrm{max}}_{4l}$ [fb]	$2.1 \cdot 10^4$	$2.9 \cdot 10^3$	$7.6 \cdot 10^3$

Table 4.1. Dimensionless parton-level proportionality factors $f_d^{g,q}, h_d^{g,q}$ and $j_d^{g,q}$, and unparticle 4γ, $2\gamma 2l$ and $4l$ reference cross sections at the LHC. The reference cross sections are calculated using $\Lambda_4 = 1$ TeV and $C_d = 1$ while the actual cross sections scale with C_d^2/Λ_d^{6d}. This quantity is bounded by Tevatron data [35], giving upper bounds on total cross sections for all final states at the LHC in question.

the Tevatron has a large density of $q\overline{q}$ pairs since it involves $p\overline{p}$ collisions, while the LHC does not.

The total cross section at the Tevatron coming from the virtual unparticle effects under discussion is

$$\sigma_{tot}^{ref} C_d^2 \left(\frac{1}{\Lambda_4\,[\mathrm{TeV}]} \right)^{6d},$$

where $\sigma_{tot}^{ref} = \sigma_{q\overline{q}\to 4\gamma}^{ref} + \sigma_{gg\to 4\gamma}^{ref}$ is the total reference cross section, determined by setting $C_d = 1$ and $\Lambda_4 = 1$ TeV. The 95 % CL upper limit of 3.04 events for zero background (the Tevatron integrated luminosity roughly yields an expected number of events equal to $3 \cdot 10^{-3}$) and zero observed events then becomes the 95 % CL bound

$$\sigma_{tot}^{ref} C_d^2 \left(\frac{1}{\Lambda_4\,[\mathrm{TeV}]} \right)^{6d} \cdot 0.83\mathrm{fb}^{-1} \leq 3.04.$$

The resulting upper bounds on $C_d/(\Lambda_4\,[\mathrm{TeV}])^{3d}$ are given in Table 4.2.2. It is important to remember that these bounds, and hence the bounds on the LHC cross

section, only apply for the values of the dimensionless coupling constants chosen here. For different values of the couplings, the maximum allowed cross sections will be different.

4.2.4 Two Photon and Two Lepton Final States

Simply replacing two of the photons with one lepton-antilepton pair yields the subprocesses $gg \to \gamma\gamma l\overline{l}$ and $q\overline{q} \to \gamma\gamma l\overline{l}$ with squared amplitudes

$$\overline{\left|\mathcal{M}_{gg\to 2\gamma l\overline{l}}\right|^2} = 64\frac{c_\gamma^2 c_g^2 e^2 (c_4^f)^2}{\Lambda_4^{6d}} v^2 (p_a\cdot p_b)^2 (p_1\cdot p_2)^2 (p_3\cdot p_4)\left|\Gamma_3(q_2,q_3)\right|^2, \tag{4.4}$$

$$\overline{\left|\mathcal{M}_{q\overline{q}\to 2\gamma l\overline{l}}\right|^2} = \frac{32}{3}\frac{c_\gamma^2 e^4 (c_4^f)^4}{\Lambda_4^{6d}} v^4 (p_a\cdot p_b)(p_1\cdot p_2)^2 (p_3\cdot p_4)\left|\Gamma_3(q_2,q_3)\right|^2, \tag{4.5}$$

respectively. These expressions should be multiplied with $(1/2!)^2$ to account for the identical particles in the final state. Just as in the four photon case, the partonic cross sections can be written as

$$\hat{\sigma}(\hat{s})_{gg\to 2l2\gamma} = h_d^g C_d^2 \left(\frac{\hat{s}}{\Lambda_4}\right)^{3d}\left(\frac{v^2}{\hat{s}}\right)\frac{1}{\hat{s}/[\mathrm{GeV}^2]}[\mathrm{fb}],$$

$$\hat{\sigma}(\hat{s})_{q\overline{q}\to 2l2\gamma} = h_d^q C_d^2 \left(\frac{\hat{s}}{\Lambda_4}\right)^{3d}\left(\frac{v^2}{\hat{s}}\right)^2\frac{1}{\hat{s}/[\mathrm{GeV}^2]}[\mathrm{fb}],$$

where the proportionality factors are also given in Table 4.2.2. The same procedure as in the four photon case also yields the reference and maximum cross sections at the LHC, as well as the p_T-distributions (Table 4.2.2). Note that the transverse momenta of all the particles are recorded and then ordered without regard of particle type, i.e., no distinction is made between the photons and leptons in this regard.

The p_T-distributions (Fig. 4.3) in this case are softer than the corresponding (same d) ones for four photons. This is of course due to the (slightly) different squared amplitudes. Since $p_1\cdot p_2 \sim E_1 E_2$ for a fixed angle between the two particles, the amplitude will increase more slowly in the high-p_T region as well. Also, since the partonic cross sections increase more slowly with $\hat{s}$ than for photons, high energy partons will contribute less. Just as in the four photon case, almost perfect agreement between the distributions from the gg and $q\overline{q}$ initial states are found.

In analogy with the four photon case, since the unparticle field is assumed to couple to quarks and gluons, one should also find $q\overline{q}gg$, $q\overline{q}\gamma\gamma$ and $l\overline{l}gg$ final states with identical spectra but larger cross sections.

4.2.5 Four Lepton Final States

For four (charged) leptons in the final state, the squared amplitudes are

$$\overline{|\mathcal{M}_{gg\to 4l}|^2} = 4\frac{c_g^2 e^4 (c_4^f)^4}{\Lambda_4^{6d}} v^4 (p_a\cdot p_b)^2 (p_1\cdot p_2)(p_3\cdot p_4)\left|\Gamma_3(q_2,q_3)\right|^2, \tag{4.6}$$

$$\overline{\left|\mathcal{M}_{q\overline{q}\to l_1\overline{l}_1 l_2\overline{l}_2}\right|^2} = \frac{2}{3}\frac{e^6 (c_4^f)^6}{\Lambda_4^{6d}} v^6 (p_a\cdot p_b)(p_1\cdot p_2)(p_3\cdot p_4)\left|\Gamma_3(q_2,q_3)\right|^2, \tag{4.7}$$

respectively. Since the τ lepton is too unstable to make it to the detector before it decays, the interesting cases are the $4e$, 4μ and $2e2\mu$ final states. In the first two cases one should include a factor of $1/4!$ and in the last $(1/2!)^2$. The cross sections in Table 4.2.2 are for the $4e$ and 4μ final states. The partonic cross sections are

$$\hat{\sigma}(\hat{s})_{gg\to 4l} = j_d^g C_d^2 \left(\frac{\hat{s}}{\Lambda_4}\right)^{3d}\left(\frac{v^2}{\hat{s}}\right)^2 \frac{1}{\hat{s}/[\mathrm{GeV}^2]}[\mathrm{fb}],$$

$$\hat{\sigma}(\hat{s})_{q\overline{q}\to 4l} = j_d^q C_d^2 \left(\frac{\hat{s}}{\Lambda_4}\right)^{3d}\left(\frac{v^2}{\hat{s}}\right)^3 \frac{1}{\hat{s}/[\mathrm{GeV}^2]}[\mathrm{fb}],$$

while the p_T-distributions are shown in Fig. 4.4. As expected, the spectra are now even softer than for the $\gamma\gamma l\overline{l}$ final state.

4.2.6 Missing Transverse Momentum

The couplings of SM neutrinos to a scalar unparticle field are usually taken as [44–47]

$$\frac{\lambda^{ab}}{\Lambda_3^{d-1}}\overline{\nu}_a\nu_b\mathcal{O}, \tag{4.8}$$

where $a,b = e,\mu,\tau$ are flavor indices. For flavor conserving couplings, λ is of course diagonal. This can lead to decay of heavy neutrinos to lighter ones [44] and other interesting phenomenological consequences. Here, however, the focus will be at processes such as

$$pp \to l^+l^-\nu\overline{\nu}, \gamma\gamma\nu\overline{\nu}.$$

The couplings in Eq. (4.8) will lead to the same squared amplitudes as in Eqs. (4.6) and (4.4), up to an overall factor.

One cannot say anything about the total cross section for these kind of processes unless one has knowledge about the couplings λ^{ab}. For λ^{ab} of the order of one and Λ_3 of the order of 1 TeV, the resulting cross sections would be of the same order of magnitude as the ones for the four charged lepton channel in the previous section. Regardless of the total cross section, one can use the events generated for the charged lepton cases to plot the distribution of missing transverse momentum, $\not{p}_T$, for 2γ and l^+l^- events at the LHC. These distributions are plotted in Figs. 4.5 and 4.6 where the additional cut $\not{p}_T > 15\,\mathrm{GeV}$ has been imposed.

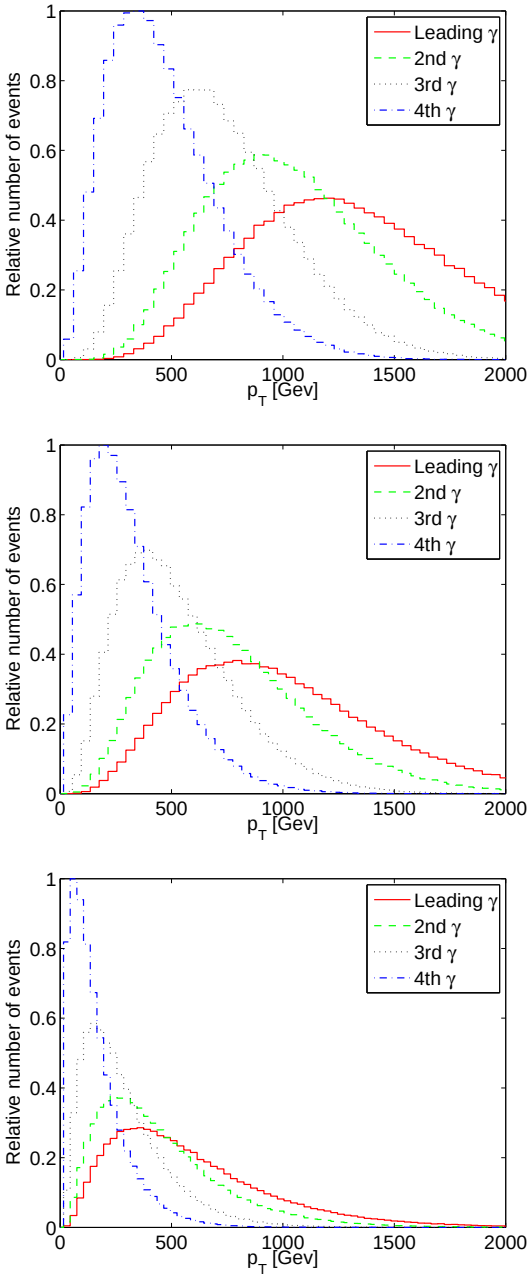

Figure 4.2. p_T distributions of p_T-ordered photons in unparticle 4γ events at the LHC for $d = 1.9$ (top), $d = 1.5$ (middle) and $d = 1.1$ (bottom).

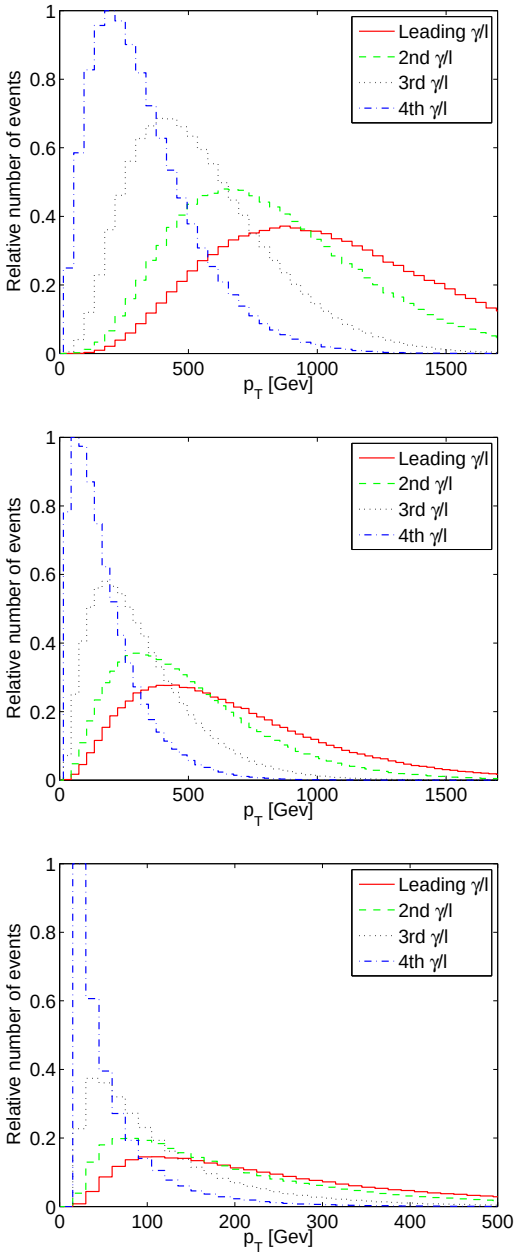

Figure 4.3. p_T distributions of p_T-ordered photons and leptons in unparticle $2\gamma 2l$ events at the LHC for $d = 1.9$ (top), $d = 1.5$ (middle) and $d = 1.1$ (bottom). Note the different scales on the p_T-axes as compared to Fig. 4.2.

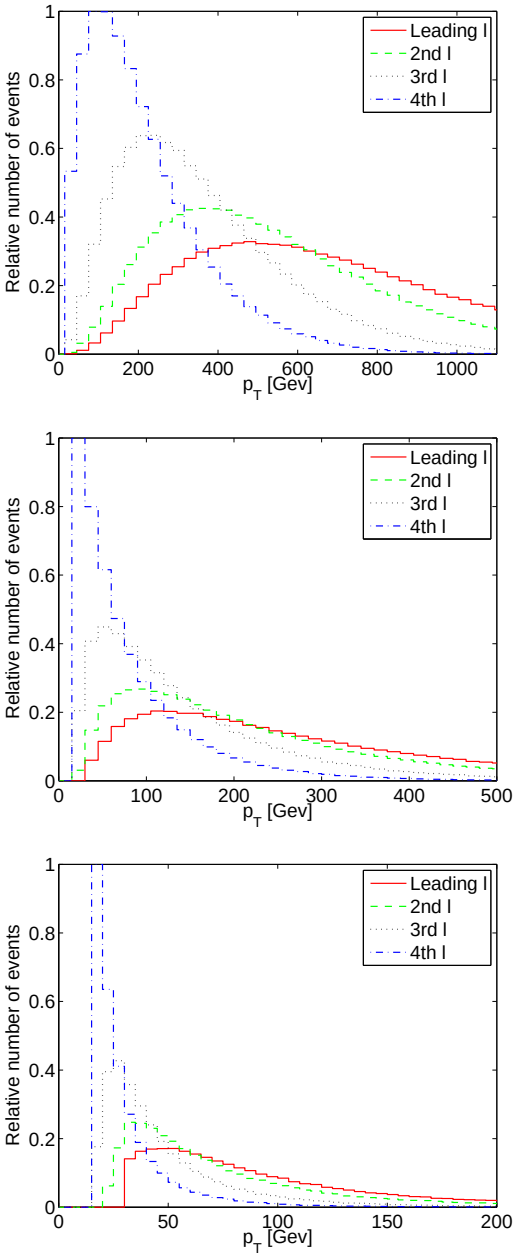

Figure 4.4. p_T distributions of p_T-ordered leptons in unparticle $4l$ events at the LHC for $d = 1.9$ (top), $d = 1.5$ (middle) and $d = 1.1$ (bottom). Note the different scales on the p_T-axes as compared to Figs. 4.2 and 4.3.

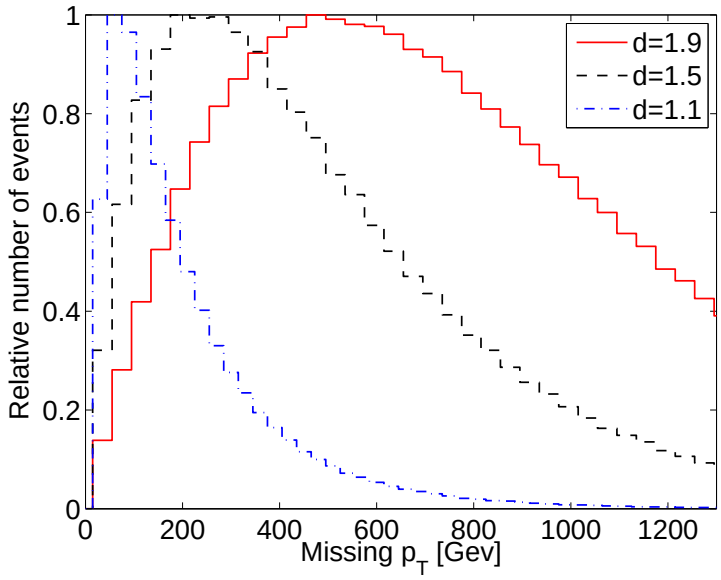

Figure 4.5. Missing transverse momentum in unparticle $l^+l^-\nu\overline{\nu}$ events at the LHC for different values of the scaling dimension.

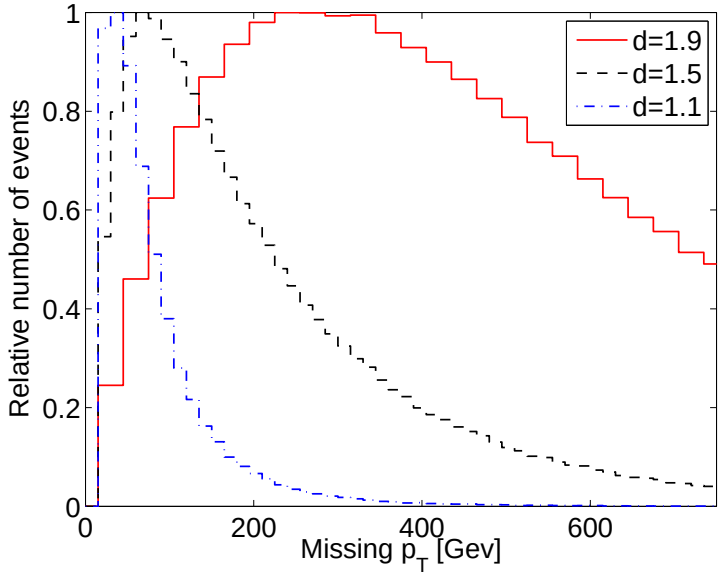

Figure 4.6. Missing transverse momentum in unparticle $2\gamma\nu\overline{\nu}$ events at the LHC for different values of the scaling dimension.

Chapter 5

Summary and Conclusions

Unparticle physics is a relatively new idea for an extension of the Standard Model of particle physics, introduced by Georgi in 2007 [25]. The basic idea is that there might exist a hidden conformal sector which is coupled to the Standard Model through effective operators. Unparticle physics is then the study of the phenomenological consequences of the SM interactions with the hidden sector.

In the beginning of this thesis, the required background material concerning conformal and effective field theory was discussed. Then, the unparticle model and how it leads to observable consequences, either through production or virtual effects, was described. Finally, the implications of the unparticle self-interactions, entering through the three-point function, for LHC phenomenology was studied. The final states examined were the 4γ, $2\gamma 2l$ and $4l$ final states, the first of which was studied in a previous publication [35]. The results take the form of upper bounds on the LHC cross sections, distributions of transverse momentum and missing transverse momentum. The allowed cross sections are observed to be large, in the range of $10^3 - 10^6$ fb. The p_T-distributions are observed to become softer with increasing number of fermions in the final state and decreasing scaling dimension of the unparticle sector. If there was to be an excess of events of the relevant final states at the LHC (possibly enormous), unparticle physics would be one possible explanation. The computed distributions could then potentially be used to identify unparticles as the source, as well as the correct value of the scaling dimension d.

The constraints on the unparticle self-interaction strength from the 4γ channel at the Tevatron was derived in Ref. [35] and used in this thesis to give upper bounds on the cross sections for the $2\gamma 2l$ and $4l$ channels. One obvious extension to the work presented in this thesis would be the derivation of similar bounds coming from the two other channels at the Tevatron. It would also be interesting to have a detailed calculation of the expected cross sections coming from SM processes only for all the final states at the LHC. Finally, one could calculate other distributions different from the ones of p_T, which could be used to identify the existence of the unparticle sector and its scaling dimension when LHC data becomes available.

Bibliography

[1] E. Wigner, *The Unreasonable Effectiveness of Mathematics in the Natural Sciences*, Communications in Pure and Applied Mathematics **13** (1960).

[2] A. Einstein, *Physics and Reality*, Journal of the Franklin Institute (1936).

[3] M. Tegmark, *The Mathematical Universe*, Found. Phys. **38**, 101 (2008), 0704.0646.

[4] P. Di Francesco, P. Mathieu and D. Senechal, *Conformal Field Theory*, New York, USA: Springer (1997) 890 p.

[5] G. Mack and A. Salam, *Finite Component Field Representations of the Conformal Group*, Ann. Phys. **53**, 174 (1969).

[6] H. Osborn and A. C. Petkou, *Implications of Conformal Invariance in Field Theories for General Dimensions*, Ann. Phys. **231**, 311 (1994), hep-th/9307010.

[7] B. Grinstein, K. A. Intriligator and I. Z. Rothstein, *Comments on Unparticles*, Phys. Lett. **B662**, 367 (2008), 0801.1140.

[8] P. Gaete and E. Spallucci, *Un-particle Effective Action*, Phys. Lett. **B661**, 319 (2008), 0801.2294.

[9] H. Nikolic, *Unparticle as a Particle with Arbitrary Mass*, Mod. Phys. Lett. **A23**, 2645 (2008), 0801.4471.

[10] H. Georgi, *Another Odd Thing about Unparticle Physics*, Phys. Lett. **B650**, 275 (2007), 0704.2457.

[11] K. Cheung, W. Y. Keung and T. C. Yuan, *Collider Phenomenology of Unparticle Physics*, Phys. Rev. **D76**, 055003 (2007), 0706.3155.

[12] G. Cacciapaglia, G. Marandella and J. Terning, *Colored Unparticles*, JHEP **01**, 070 (2008), 0708.0005.

[13] A. Rajaraman, *Aspects of Unparticle Physics*, AIP Conf. Proc. **1078**, 63 (2009), 0809.5092.

[14] R. Zwicky, *Unparticles and CP-violation*, J. Phys. Conf. Ser. **110**, 072050 (2008), 0710.4430.

[15] E. P. Wigner, *On Unitary Representations of the Inhomogeneous Lorentz Group*, Annals Math. **40**, 149 (1939).

[16] G. Mack, *All Unitary Ray Representations of the Conformal Group SU(2,2) with Positive Energy*, Commun. Math. Phys. **55**, 1 (1977).

[17] J. Polchinski, *Scale And Conformal Invariance in Quantum Field Theory*, Nucl. Phys. **B303**, 226 (1988).

[18] T. Banks and A. Zaks, *On the Phase Structure of Vector-Like Gauge Theories with Massless Fermions*, Nucl. Phys. **B196**, 189 (1982).

[19] D. D. Dietrich and F. Sannino, *Conformal Window of SU(N) Gauge Theories with Fermions in Higher Dimensional Representations*, Phys. Rev. **D75**, 085018 (2007), hep-ph/0611341.

[20] F. Sannino, *Conformal Chiral Dynamics*, (2008), 0811.0616.

[21] H. Georgi and Y. Kats, *An Unparticle Example in 2D*, Phys. Rev. Lett. **101**, 131603 (2008), 0805.3953.

[22] T. A. Ryttov and F. Sannino, *Conformal Windows of SU(N) Gauge Theories, Higher Dimensional Representations and the Size of the Unparticle World*, Phys. Rev. **D76**, 105004 (2007), 0707.3166.

[23] A. Pich, *Effective field theory*, (1998), hep-ph/9806303.

[24] A. V. Manohar, *Effective field theories*, (1996), hep-ph/9606222.

[25] H. Georgi, *Unparticle Physics*, Phys. Rev. Lett. **98**, 221601 (2007), hep-ph/0703260.

[26] M. Bander *et al.*, *Unparticles: Scales and High Energy Probes*, Phys. Rev. **D76**, 115002 (2007), 0706.2677.

[27] S. L. Chen and X. G. He, *Interactions of Unparticles with Standard Model Particles*, Phys. Rev. **D76**, 091702 (2007), 0705.3946.

[28] M. Neubert, *Unparticle Physics with Jets*, Phys. Lett. **B660**, 592 (2008), 0708.0036.

[29] A. Rajaraman, *On the Decay of Unparticles*, (2008), 0806.1533.

[30] A. Delgado *et al.*, *A Note on Unparticle Decays*, (2008), 0812.1170.

[31] K. Cheung, W. Y. Keung and T. C. Yuan, *Unparticle Phenomenology – A Mini Review*, AIP Conf. Proc. **1078**, 156 (2009), 0809.0995.

[32] P. J. Fox, A. Rajaraman and Y. Shirman, *Bounds on Unparticles from the Higgs Sector*, Phys. Rev. **D76**, 075004 (2007), 0705.3092.

[33] J. P. Lee, *Deconstructing Unparticles in Higher Dimensions*, (2009), 0901.1020.

[34] G. von Gersdorff and M. Quiros, *Conformal Neutrinos: An Alternative to the See-Ssaw Mechanism*, (2009), 0901.0006.

[35] J. L. Feng, A. Rajaraman and H. Tu, *Unparticle Self-Interactions and Their Collider Implications*, Phys. Rev. **D77**, 075007 (2008), 0801.1534.

[36] M. J. Strassler, *Why Unparticle Models with Mass Gaps are Examples of Hidden Valleys*, (2008), 0801.0629.

[37] T. Han, *Collider Phenomenology: Basic Knowledge and Techniques*, (2005), hep-ph/0508097.

[38] J. Pumplin *et al.*, *New Generation of Parton Distributions with Uncertainties from Global QCD Analysis*, JHEP **07**, 012 (2002), hep-ph/0201195.

[39] CompHEP, E. Boos *et al.*, *CompHEP 4.4: Automatic Computations from Lagrangians to Events*, Nucl. Instrum. Meth. **A534**, 250 (2004), hep-ph/0403113.

[40] A. Pukhov *et al.*, *CompHEP: A Package for Evaluation of Feynman Diagrams and Integration over Multi-Particle Phase Space. User's Manual for Version 33*, (1999), hep-ph/9908288.

[41] G. P. Lepage, *A New Algorithm for Adaptive Multidimensional Integration*, J. Comput. Phys. **27**, 192 (1978).

[42] E. Eichten, K. D. Lane and M. E. Peskin, *New Tests for Quark and Lepton Substructure*, Phys. Rev. Lett. **50**, 811 (1983).

[43] D. Collaboration, *D0 Note 5067-CONF*.

[44] S. Zhou, *Neutrino Decays and Neutrino Electron Elastic Scattering in Unparticle Physics*, Phys. Lett. **B659**, 336 (2008), 0706.0302.

[45] J. Barranco *et al.*, *Unparticle Physics and Neutrino Phenomenology*, (2009), 0901.2099.

[46] D. Montanino, M. Picariello and J. Pulido, *Probing Neutrino Magnetic Moment and Unparticle Interactions with Borexino*, Phys. Rev. **D77**, 093011 (2008), 0801.2643.

[47] A. B. Balantekin and K. O. Ozansoy, *Constraints on Unparticles from Low Energy Neutrino- Electron Scattering*, Phys. Rev. **D76**, 095014 (2007), 0710.0028.